Arabidopsis Poly(ADP-ribose)-binding protein RCD1 interacts with Photoregulatory Protein Kinases in nuclear bodies.

Julia P. Vainonen[1,2]*, Alexey Shapiguzov[1,3]*, Julia Krasensky-Wrzaczek[1]*, Raffaella De Masi[4,5], Richard Gossens[1], Iulia Danciu[6,7], Natalia Battchikova[8], Claudia Jonak[6,7], Lennart Wirthmueller[4,5], Michael Wrzaczek[1], Jaakko Kangasjärvi[1]

Author affiliations

1. Organismal and Evolutionary Biology Research Programme, Faculty of Biological and Environmental Sciences, and Viikki Plant Science Center, University of Helsinki, FI-00014 Helsinki, Finland.

2. Current address: Turku Bioscience Centre, University of Turku, FI-20520 Turku, Finland

3. Permanent address: Institute of Plant Physiology, Russian Academy of Sciences, Botanicheskaya Street, 35, 127276 Moscow, Russia.

4. Department Biochemistry of Plant Interactions, Leibniz Institute of Plant Biochemistry, Weinberg 3, 06120 Halle (Saale), Germany

5. Dahlem Centre of Plant Sciences, Institute of Biology, Freie Universität Berlin, Königin-Luise-Str. 12-16, 14195 Berlin, Germany

6. Gregor Mendel Institute, Austrian Academy of Sciences, Vienna BioCenter, Dr. Bohr-Gasse 3, 1030 Vienna, Austria

7. Bioresources Unit, Center for Health & Bioresources, AIT Austrian Institute of Technology GmbH, 3430, Tulln, Austria.

8. Department of Biochemistry, Molecular Plant Biology, University of Turku, FI-20014 Turku, Finland.

* These authors contributed equally to the manuscript.

Corresponding author: Jaakko Kangasjärvi, jaakko.kangasjarvi@helsinki.fi

Abstract

Continuous reprograming of gene expression in response to environmental signals in plants is achieved through signaling hub proteins that integrate external stimuli and transcriptional responses. RADICAL-INDUCED CELL DEATH1 (RCD1) functions as a nuclear hub protein, which interacts with a variety of transcription factors with its C-terminal RST domain and thereby acts as a co-regulator of numerous plant stress reactions. Here a previously function for RCD1 as a novel plant PAR reader protein is shown; RCD1 functions as a scaffold protein, which recruits transcription factors to specific locations inside the nucleus in PAR-dependent manner. The N-terminal WWE- and PARP-like domains of RCD1 bind poly(ADP-ribose) (PAR) and determine its localization to nuclear bodies (NBs), which is prevented by chemical inhibition of PAR synthesis. RCD1 also binds and recruits Photoregulatory Protein Kinases (PPKs) to NBs. The PPKs, which have been associated with circadian clock, abscisic acid, and light signaling pathways, phosphorylate RCD1 at multiple sites in the intrinsically disordered region between the WWE- and PARP-like-domains, which affects the stability and function of RCD1 in the nucleus. Phosphorylation of RCD1 by PPKs provides a mechanism where turnover of a PAR-binding transcriptional co-regulator is controlled by nuclear phosphorylation signaling pathways.

INTRODUCTION

Plants are constantly exposed to a variety of environmental cues that are relayed to the nucleus leading to changes in gene expression. The eukaryotic nucleus has many functions including DNA and RNA biogenesis and processing, transcriptional regulation, RNA splicing, protein modification and degradation. These functions are organized within non-membranous compartments, so-called "nuclear bodies" (NBs; Mao *et al*, 2011). Several NBs have been identified, including the nucleolus, Cajal bodies, Polycomb bodies, and photobodies. NB-associated proteins have been described, including members of the splicing machinery (Reddy *et al*, 2012), chromatin-associated proteins (Simon *et al*, 2015), ubiquitin ligases (Christians *et al*, 2012), photoreceptors (Van Buskirk *et al*, 2012), and protein kinases (Wang *et al*, 2015).

Arabidopsis thaliana RADICAL-INDUCED CELL DEATH1 (RCD1) is a nuclear-localized multidomain protein comprised of an N-terminal bipartite nuclear localization sequence (NLS), a WWE-domain, a poly(ADP-ribose) polymerase-like (PARP-like)-domain, and an RCD1-SRO-TAF4 (RST)-domain (Ahlfors *et al*, 2004; Jaspers *et al*, 2009; Jaspers *et al*, 2010; **Figure 1A**). The inter-domain regions of RCD1 are intrinsically disordered regions (IDRs), which likely provides flexibility in assuming the final overall protein conformation. RCD1 and its paralog, SRO1 (SIMILAR TO RCD ONE 1), can form homo- and heterodimers (Wirthmueller *et al*, 2018) and can be considered essential proteins since the *rcd1 sro1* double mutant is not viable under standard growth conditions (Jaspers *et al*, 2009; Teotia & Lamb, 2011). In plants, the RST-domain is unique to the RCD1-SRO protein family and TAF4 proteins (Jaspers *et al*, 2010). It has been described as a domain that mediates interactions with many RCD1-associated proteins (O'Shea *et al*, 2017; Bugge *et al*, 2018; Shapiguzov *et al*, 2019). A structurally diverse set of transcription factors interacts with the RST-domain, making RCD1 an important hub of transcriptional regulation (Jaspers *et al*, 2009; Vainonen *et al*, 2012; O'Shea *et al*, 2017; Christensen *et al*, 2019; Shapiguzov *et al*, 2019; Jespersen & Barbar, 2020). Unlike the RST-domain, the WWE- and PARP-like-domains of RCD1 have hardly been characterized. The WWE-domain was originally proposed to be a protein-protein interaction domain related to ubiquitination and ADP-ribosylation (Aravind 2001). Later studies have shown that animal WWE-domains bind iso-ADP ribose (a structural unit of poly(ADP-ribose) - PAR; Wang *et al*, 2012; DaRosa *et al*, 2015). In *Arabidopsis thaliana*, the WWE-domain has only been found in RCD1 and its paralog SRO1. While the PARP-like-domain in these proteins does not have PARP activity (Jaspers *et al*, 2010;

Wirthmueller *et al*, 2018), the presence of a WWE- and a PARP-like-domains together suggests a function of RCD1 in PAR-related processes (Vainonen *et al*, 2016).

Poly-ADP-ribosylation (PARylation) of proteins is a reversible posttranslational modification, which has so far been mostly studied in animals (Gupte *et al*, 2017; Cohen & Chang, 2018). PARPs catalyze PARylation by covalently attaching ADP-ribose moieties to glutamate, aspartate, lysine, arginine, serine, threonine and cysteine residues in a species- and tissue-specific manner (Jungmichel *et al*, 2013; Zhang *et al*, 2013; Martello *et al*, 2016; Leung 2017; Palazzo *et al*, 2018). PAR-glycohydrolase (PARG) can trim down PAR chains to the terminal protein-bound ADP-ribose thereby removing PAR from proteins. Additionally, several signaling components that recognize PARylated proteins, so-called "PAR readers", have been identified in animal systems (Gupte *et al*, 2017; Kim *et al*, 2020) but have not been described in plants yet. On a functional level, PARylation has been shown to regulate a variety of cellular processes including chromatin remodeling, transcription, and programmed cell death (Gupte *et al*, 2017; Kim *et al*, 2020). In plants, the role of PAR is only starting to emerge: the few studies available suggest an important role for PARylation in plant stress and developmental responses (Vainonen *et al*, 2016).

In addition to transcription factors, RCD1 has been shown to interact with Photoregulatory Protein Kinases (PPKs; also named MUT9-like kinases, MLKs, or Arabidopsis EL1-like kinases, AELs; Wirthmueller *et al*, 2018; Shapiguzov *et al*, 2019). In Arabidopsis, this recently discovered protein kinase family is comprised of 4 members that have been shown to localize to NBs (Wang *et al*, 2015). PPKs interact with different nuclear proteins, including histones, components of the circadian clock and light signaling, and the ABA receptor PYR/PYL/RCAR (Wang *et al*, 2015; Huang *et al*, 2016; Liu *et al*, 2017; Ni *et al*, 2017; Su *et al*, 2017; Chen *et al*, 2018; Zheng *et al*, 2018). While the mechanistic role of histone and circadian clock component phosphorylation by PPKs has not been described, phosphorylation of the transcription regulators PIF3 and CRY2, and the ABA receptor PYR/PYL/RCAR has been shown to target these proteins for degradation (Liu *et al*, 2017; Ni *et al*, 2017; Chen *et al*, 2018).

Here we show that Arabidopsis RCD1 localizes to NBs in a PAR-dependent manner. RCD1 directly binds PAR via the WWE- and PARP-like-domains and can therefore be described as the first identified PAR reader in plants. Furthermore, we demonstrate that RCD1 is phosphorylated by PPK protein kinase family members, which co-localize with RCD1 *in vivo* in NBs. Increased RCD1 protein levels

together with altered tolerance to oxidative stress in *ppk* mutant plants suggest that phosphorylation by PPKs regulates RCD1 protein stability.

RESULTS

Nuclear localization is essential for RCD1 function

To address the role of RCD1 localization for its function, the basic amino acids of the NLS were substituted with aliphatic ones (K21L/R22I and R56I/R57I). These point mutations were introduced into a construct expressing RCD1 tagged with triple HA epitope at the protein C-terminus, under the native RCD1 promoter (Jaspers *et al*, 2009) and expressed in *rcd1* background (RCD1*nls*-HA lines hereafter). Among other stress- and development-related phenotypes (Overmyer *et al*, 2000; Ahlfors *et al*, 2004; Jaspers *et al*, 2009; Teotia & Lamb, 2009; Hiltscher *et al*, 2014), the *rcd1* mutant displays curly leaves and tolerance to the herbicide methyl viologen (MV) (Ahlfors *et al*, 2004; Fujibe *et al*, 2004; Shapiguzov *et al*, 2019). At the molecular level, MV interferes with the electron transfer chain in chloroplasts and catalyzes production of reactive oxygen species (ROS). Introduction of RCD1*nls*-HA into *rcd1* did not complement the curly leaf phenotype whereas RCD1-HA restored the leaf phenotype (**Figure 1B**). Similarly, the increased tolerance of *rcd1* to MV was not reverted to wild type-like sensitivity in RCD1*nls*-HA plants (**Figure 1C**). Analysis of RCD1 protein levels in the transgenic lines revealed increased RCD1 accumulation in RCD1*nls*-HA lines compared to wild type RCD1-HA (**Figure 1D**). Thus, despite higher levels of RCD1 in RCD1*nls*-HA lines, *rcd1* phenotypes were not complemented. These results suggest that nuclear localization is required for the proper function of RCD1.

RCD1 localizes to NBs and binds PAR

To study the subcellular localization of RCD1 in further detail, we generated stable Arabidopsis lines expressing wild type RCD1-Venus fusion protein, as well as deletion constructs lacking the individual domains (WWE, PARP-like, and RST) under control of the *UBIQUITIN10* promoter in *rcd1* background. A schematic representation of RCD1-Venus constructs is shown in **Supplementary figure 1A**. Wild type RCD1-Venus and the domain deletion mutants complemented the *rcd1* mutant habitus (**Supplementary figure 1B**), confirming that the introduced transgenes retained functionality. The MV sensitivity phenotype was restored by RCD1-Venus, the RCD1ΔWWE-Venus and

RCD1ΔPARP-Venus constructs but only partially by RCD1ΔRST-Venus (**Supplementary figure 1C**), suggesting that the RST-domain is essential for at least some of the several functions of RCD1.

Microscopic analysis of wild type RCD1-Venus lines showed that RCD1 localized exclusively to the nucleus. Within the nucleus, RCD1-Venus localized to the nucleoplasm and, interestingly, in distinct NBs (**Figure 2A**). Deletion of the WWE- or the PARP-like-domain eliminated the localization of RCD1 to these NBs under standard growth conditions, whereas its nuclear distribution was not influenced by the deletion of the RST-domain (**Figure 2A**). Immunoblot analysis of the corresponding lines showed increased levels of RCD1 in all deletion construct lines compared to wild type RCD1-Venus (**Supplementary figure 1D**). Thus, disappearance of RCD1 from NBs was not due to low protein abundance.

The WWE-domain has previously been described to bind PAR in mammalian cells (Zhang *et al*, 2011; Wang *et al*, 2012; DaRosa *et al*, 2015). Therefore, we tested whether 3-methoxybenzamide (3MB), a chemical inhibitor of PAR synthesis, would influence NB localization of RCD1-Venus. Indeed, in 3MB-treated plants, RCD1-Venus appeared almost exclusively in the nucleoplasm (**Figure 2B**). This suggests that the presence of PARylated proteins in the nucleus would be necessary for RCD1 to localize to NBs.

To examine whether RCD1 can bind PAR directly, we tested the interaction *in vitro*. Recombinant proteins were expressed in *E. coli*, purified (**Supplementary Figure 2A**) and dot-blotted on a nitrocellulose membrane. The membrane was then incubated with PAR polymer, washed, and subsequently probed with anti-PAR or anti-GST antibodies. As shown in **Figure 2C**, the WWE-domain of RCD1 alone, as well as the full-length protein (fused to either GST or His-tags, respectively), interacted with PAR. Interestingly, the affinity to PAR was stronger for full-length RCD1 compared to the WWE-domain alone (**Figure 2C**). This suggests that the PARP-like-domain of RCD1 was also involved in PAR binding *in vitro*. To verify that PAR-binding was mediated by the WWE-domain, we tested the PAR-binding properties of a truncated version of RCD1 lacking the WWE-domain (GST-RCD1ΔWWE), which was not able to bind PAR as shown in **Figure 2C**.

For quantitative characterization of the RCD1-PAR interaction we applied surface plasmon resonance (SPR), a method which allows label-free detection of biomolecular interactions. SPR demonstrated that full-length RCD1 interacted with PAR and that the interaction was abolished by deletion of the WWE-domain (GST-RCD1ΔWWE; **Figure 2D**). The binding curve was congruent with the WWE-domains

described in other studies (Zhang *et al*, 2011; Wang *et al*, 2012). Absence of dissociation in the running buffer (**Figure 2D**) confirmed strong complex formation between PAR and RCD1. Estimation of the affinity of the interaction by binding experiments with increasing concentrations of the PAR ligand resulted in a dissociation constant of 28.2 nM (**Supplementary Figure 2D**). However, SPR analyses did not identify interaction between RCD1 and compounds related to PAR, monomeric ADP-ribose or cyclic ADP-ribose, a known second messenger (**Supplementary Figure 2B** and **C**). Thus, our experiments showed that RCD1 binds PAR with specificity, high affinity and this interaction requires the WWE- and PARP-like- domains.

RCD1 colocalizes with PPKs in NBs

Immunoblot analyses showed that nuclear-localized RCD1-HA migrated in SDS-PAGE as a double band (**Figure 1D**), indicative of post-translational modification of the protein. To test whether the double band was caused by phosphorylation of RCD1, protein extracts from plants expressing wild type RCD1-HA were treated with calf intestinal alkaline phosphatase (CIP). The phosphatase treatment eliminated the double band of RCD1-HA (**Supplementary Figure 3**), suggesting that RCD1 is an *in vivo* phosphoprotein. RCD1-HA migrated as a single band in the transgenic lines expressing RCD1*nls*-HA (**Figure 1D**), indicating that nuclear localization was necessary for phosphorylation of RCD1.

Our previous proteomic analyses of RCD1-interactors (Wirthmueller *et al*, 2018; Shapiguzov *et al*, 2019), showed that RCD1 interacted *in vivo* with a newly described family of protein kinases, the Photoregulatory Protein Kinases (PPKs). This interaction was confirmed by targeted co-immunoprecipitation experiments in tobacco using RCD1-GFP and PPK-HA constructs, in which RCD1-GFP co-immunoprecipitated with PPK1, 3 and 4 (**Supplementary Figure 4**). The apparent lack of interaction between RCD1 and PPK2 in this assay could indicate either isoform-specific differences in the strength of association, or represented a technical limitation as PPK2 protein was hardly detectable in total protein extracts. Collectively, these data confirmed complex formation between RCD1 and PPKs also in a heterologous expression system.

It has previously been shown that PPKs localize to NBs in Arabidopsis (Wang *et al*, 2015). To test whether PPKs co-localized with RCD1, we co-expressed RCD1-Venus and PPK-RFP transiently in tobacco. Results shown in **Figure 3A** demonstrated co-localization of RCD1 with all four RFP-tagged PPKs in NBs, but not with RFP alone (**Figure 3A**). Expression of PPK-RFP constructs alone in tobacco showed uniform distribution of the proteins inside the nucleus (**Figure 3B**), which suggests

that localization of PPKs to NBs was dependent on the interaction with RCD1-Venus. Thus, these results were in line with complex formation between RCD1 and PPKs and confirmed their co-localization in NBs.

RCD1 is phosphorylated by PPKs

Interaction of RCD1 with PPKs prompted us to study the phosphorylation of RCD1 in more detail. Mass spectrometric determination of *in vivo* phosphosites in RCD1-HA immunoprecipitated from Arabidopsis revealed several phospho-serine and phospho-threonine-containing peptides (**Table 1**). To verify whether PPKs could phosphorylate RCD1 directly, we tested PPK kinase activity towards RCD1 *in vitro* using recombinant GST-tagged proteins. GST-PPK2 and GST-PPK4 could be purified from *E. coli* with detectable kinase activity against the generic substrates MBP and casein (**Supplementary figure 5**). Phosphorylation experiments using radioactively labelled γ[^{32}P]-ATP (**Figure 4B**) showed that both GST-PPKs were able to directly phosphorylate GST-RCD1 *in vitro*. Phosphorylated GST-RCD1 was analyzed by mass spectrometry to identify PPK-dependent *in vitro* phosphorylation sites. This revealed that several of the PPK-dependent *in vitro* phosphopeptides of RCD1 were also identified in the *in vivo* pull-down experiments. All *in vivo* and *in vitro* phosphopeptides from this and an earlier study (Wirthmueller *et al*, 2018) are listed in **Table 1**. A schematic representation of all identified phospho-sites in RCD1 is shown in **Figure 4A**. Interestingly, RCD1 is phosphorylated almost exclusively in its IDRs.

Combined data of *in vivo* and *in vitro* analyses of RCD1 phosphorylation revealed that most phosphosites concentrated in IDR2, the region between the WWE- and PARP-like-domains. We mutated the 15 identified phosphosites in this region to non-phosphorylatable alanine residues by gene synthesis (GST-RCD1$^{S/T}$IDR2^{A}). This protein variant was subjected to *in vitro* kinase assays with GST-PPK2 and GST-PPK4. Mutation of the 15 phosphosites in IDR2 abolished phosphorylation of RCD1 by PPKs **(Figure 4B, C)**. Thus, PPKs showed specificity towards RCD1 phosphosites in IDR2. This is consistent with the previous result that the sequence up to the PARP-like-domain was sufficient to co-immunoprecipitate endogenous PPKs from plant cell extracts (Wirthmueller *et al*, 2018). To address the role of IDR2 phosphorylation *in vivo,* we generated transgenic lines expressing RCD1$^{S/T}$IDR2^{A}-HA construct in *rcd1* background under the native RCD1 promoter. Analysis of protein abundance with a HA-specific antibody revealed that in half of the *rcd1*: RCD1$^{S/T}$IDR2^{A}-HA lines (e.g. line C), RCD1 level was notably higher than in the lines expressing highest levels of wild

type RCD1 (**Figure 4D**). In accordance with the *in-vitro* data, mutation of the IDR2 phospho-sites to alanine resulted in disappearance of the phosphorylated protein form in *rcd1*: RCD1$^{S/T}$IDR2^{A}-HA line (**Supplementary figure 6**). Despite the higher abundance, the RCD1$^{S/T}$IDR2^{A}-HA variant did not fully complement *rcd1*-specific (Shapiguzov *et al*, 2019) accumulation of alternative oxidases (AOX1/2), as revealed by immunoblot with αAOX1/2 antibodies (**Figure 4D**). Neither did expression of RCD1$^{S/T}$IDR2^{A}-HA expression fully complement the *rcd1* MV tolerance (**Figure 4E**), which suggests that mutation of the 15 residues in IDR2 affect the nuclear function of RCD1.

In addition to the PPK-related phospho-sites between the WWE- and the PARP-like-domains, RCD1 contains other *in vivo* phosphorylation sites, presumably targeted by other protein kinases linking RCD1 to different upstream signaling pathways **(Figure 4A)**. One of the identified sites, Thr204, is a predicted target for proline-directed protein kinases. We tested Arabidopsis GSK3/Shaggy-like protein kinases (ASKs), a group of stress-related proline-directed protein kinases (Saidi *et al*, 2012), for their ability to phosphorylate RCD1. *In vitro* kinase assays with several ASKs (**Supplementary figure 7A**) showed that ASKα, ASKɣ, and to a lesser extent, ASKε phosphorylated RCD1. Since Thr204 was the only phosphorylated residue flanked by a proline, we mutated Thr204 to alanine (RCD1-T204A). This mutation abolished or strongly reduced phosphorylation of RCD1 by the ASKs (**Supplementary figure 7B**) indicating that ASKα, ASKɣ, and ASKε target Thr204. The kinases targeting phospho-sites towards the N- and C-termini remain to be identified.

Our results with *rcd1*: RCD1$^{S/T}$IDR2^{A}-HA lines (**Figure 4D** and **Supplementary figure 6**) suggest that phosphorylation by PPKs affects the stability of RCD1. PPK-mediated phosphorylation of proteins has been shown to impact protein stability by targeting proteins for degradation (Ni *et al*, 2016; Liu *et al*, 2017; Chen *et al*, 2018). To further address this question, we analyzed RCD1 levels in triple *ppk* mutant plants. Immunoblot analysis of *ppk124* and *ppk234* with an RCD1-specific antibody revealed increased RCD1 levels compared to wild type plants (**Figure 5A**). Furthermore, in accordance with earlier results (Shapiguzov *et al*, 2019), higher accumulation of native RCD1, such as in triple *ppk* mutants, coincided with lower resistance of plants to MV compared to wild type (**Figure 5B**). These data suggest that PPK-dependent phosphorylation of RCD1 plays an important regulatory role for RCD1 protein stability and function.

DISCUSSION

Plants continuously reprogram their gene expression in response to environmental stimuli. In nature, numerous simultaneous signals and cues have to be processed and integrated to achieve an adequate and balanced response. This can be accomplished e.g., with hub proteins which integrate signals from different sources and adjust the activity of transcription factors to ensure appropriate responses (Bugge *et al*, 2018; Vandereyken *et al*, 2018; Jespersen & Barbar, 2020). Hub proteins frequently interact with many different protein partners, including transcription factors, to provide a flexible system which can simultaneously adjust several cellular functions according to changes in the surrounding environment. The RCD1 protein has been suggested in several studies to be such a hub protein (Jaspers *et al*, 2009; Hiltscher *et al*, 2014, Bugge *et al*, 2018; Shapiguzov *et al*, 2019; Jespersen & Barbar, 2020). Accordingly, disruption of the *RCD1* gene results in highly pleiotropic phenotypes and altered expression of a large number of genes (Ahlfors *et al*, 2004; Jaspers *et al*, 2009; Teotia & Lamb 2009, Brosché *et al*, 2014). Interaction of RCD1 with such a great variety of proteins is facilitated by its IDRs (IDR3 and IDR4), which enable RCD1 to adjust its final conformation upon binding to its interaction partners (Kragelund *et al*, 2012; O'Shea *et al*, 2017). In addition, other factors, such as recognition of signaling molecules or regulation of protein stability can contribute to the versatility of hub proteins, including RCD1.

RCD1 and PARylation

Protein PARylation is a transient post-translational modification that has been associated with adjustment of development and response to stress conditions in plants (Briggs & Bent, 2011; Lamb *et al*, 2012; Feng *et al*, 2015). While the inventories of PARPs and PARGs have been defined in Arabidopsis (Vainonen *et al*, 2016; Rissel & Peiter, 2019), so far only a limited number of proteins have been reported to be PARylated in plants. These include PARPs (Babiychuk *et al*, 1998; Feng *et al*, 2015), histones (Whitby *et al*, 1979; Willmitzer 1979) and the nuclear protein DAWDLE involved in micro-RNA processing (Feng *et al*, 2016). Nuclear Cajal bodies have also been linked to active PARPs in plants (Love *et al*, 2017). The so-called "PAR readers", proteins which non-covalently bind PAR (Teloni & Altmeyer, 2016; Gupte *et al*, 2017), have thus far remained unidentified in plants. It has been suggested that the PAR polymer provides an interaction platform for PAR reader proteins to modulate cellular responses, including chromatin remodeling, protein degradation and cell death (Kim *et al*, 2020). Our biochemical analyses revealed that RCD1 binds PAR and that the interaction is mediated by

the WWE- and PARP-like-domains in a cooperative fashion. This suggests that RCD1 functions as a PAR-binding protein *in vivo*, making it a novel PAR reader protein described in plants.

In mammalian cells, PAR colocalizes with PAR-binding proteins in NBs (Ahel *et al*, 2008). The localization of RCD1 in NBs reported in this study was compromised if either the WWE- or the PARP-like-domain was removed. Furthermore, NB localization was suppressed by 3MB, a nicotinamide analog that inhibits PARP activity (**Figure 2**). Taken together, these observations suggest that localization of RCD1 to NBs was PAR-dependent. The molecular mechanisms whereby PAR participates in the formation of NBs and the recruitment of RCD1 therein, however, remain unknown. While the WWE-PARP module of RCD1 interacts with PAR, the C-terminal RST-domain of RCD1 binds many different transcription factors (Jaspers *et al*, 2009, 2010). Thus, one possible mode of RCD1 action could be the PAR-dependent recruitment of transcription factors to various nuclear locations, including PAR-dependent NBs, PARylated histones or other PARylated chromatin-associated proteins. This would make the PAR reader RCD1 a scaffold component that introduces its partner transcription factors to specific locations in the nucleus or the chromatin.

By recruiting transcription factors to PARylated chromatin components, both activation (Hiltscher *et al*, 2014) and repression (Vainonen *et al*, 2012; Shapiguzov *et al*, 2019) of these transcription factors could be achieved, depending on whether they would be brought in contact with actively transcribed chromatin, or targeted for degradation. Analysis of WWE-domain proteins in animals has shown that the WWE-domains co-exist in a protein not only with PARP-/PARP-like-domains, but also with E3 ubiquitin-ligase domains (Aravind 2001; Wang *et al*, 2012) which are involved in proteasomal degradation. Intriguingly, a significant fraction of transcription factors interacting with RCD1 are known to be regulated by proteasomal degradation (Qin *et al*, 2008; Ni *et al*, 2017; Favero *et al*, 2020). Furthermore, gene ontology analysis of altered gene expression in the *rcd1* mutant revealed enrichment in ubiquitin-proteasome-pathway associated genes (Jaspers et al 2009). This supports a functional link between RCD1 and the nuclear proteasomal apparatus in Arabidopsis and suggests an evolutionary conserved link of PARylation and PAR readers with proteasomal degradation.

Phosphorylation in RCD1 regulation

Hub proteins are often targets for multiple regulatory modifications enabling their involvement in a variety of upstream signaling processes. For example, RCD1 has recently been shown to perceive

signals from organelles through thiol redox relay (Shapiguzov *et al*, 2019). Protein phosphorylation is another example of a ubiquitous post-translational protein modification that plays a major role in almost all physiological processes (Mergner *et al*, 2020). RCD1 is an *in vivo* phosphoprotein; overall, 13 phospho-peptides harboring potentially 30 phosphosites have been identified after immunoprecipitation of RCD1 from protein extracts. Notably, these phosphosites were enriched in the IDRs at the N-terminus as well as between the WWE-, PARP-like-, and RST-domains of RCD1 (**Figure 4A**). It has been shown that protein kinases preferentially target IDRs, and that phosphorylation can trigger disorder-to-order transitions of the protein structure (Iakoucheva *et al*, 2004; Bah & Forman-Kay, 2016). For example, phosphorylation of C-terminal IDRs of RCD1 may assist protein folding or adjust its conformation to allow interaction with other proteins through the RST-domain. Structural analysis of RCD1 *in vitro* has shown that the disordered parts of the RST-domain adapt their final folding upon interaction with different transcription factors (Bugge *et al*, 2018; Shapiguzov *et al*, 2019). Additional phosphorylation of IDRs flanking the RST-domain (IDR3 and IDR4) may influence the structure of RCD1 and its interaction with transcription factors *in vivo*.

In addition to C-terminal phosphopeptides flanking the RST-domain, we identified a phosphorylation hotspot in IDR2 between the WWE- and the PARP-like-domains targeted by PPKs. IDR2 has been shown to be important for homo- or heterodimerization of RCD1 and its closest homolog SRO1 (Wirthmüller *et al*, 2018). Consequently, phosphorylation of IDR2 may affect the overall scaffolding structure of RCD1 and therefore regulate a wide variety of protein-protein interactions. In a recent study, IDR2 was reported to be required for the interaction between RCD1 and the oomycete effector protein HaRxL106 that prevents activation of plant immunity (Wirthmüller *et al*, 2018). Similarly, a *Phytophthora* RxLR effector has been shown to prevent relocalization of two tobacco NAC transcription factors from the endoplasmic reticulum to nucleus, which promoted disease progression (McLellan *et al*, 2013). Interestingly these tobacco NAC transcription factors, NTP1 and NTP2, are homologs of Arabidopsis ANAC013 and ANAC017, which are negatively regulated by RCD1 (Shapiguzov *et al*, 2019). Furthermore, it has been shown that ASKα, a potential upstream kinase of RCD1, has been contributing to plant immunity by modulating the oxidative pentose phosphate pathway (Stampfl *et al*, 2016). These results link RCD1 to the regulation of plant immunity and the phosphorylation of IDR2 appears to be involved in these processes.

It seems likely that phosphorylation of RCD1 by PPKs regulates RCD1 stability. The endogenous levels of RCD1 were higher in *ppk124* and *ppk234* triple mutants (**Figure 5A**) and in transgenic plants where *rcd1* was complemented with the (RCD1$^{S/T}$IDR2^{A}) construct (**Figure 4D**). Accordingly, the *ppk124* and *ppk234* triple mutants exhibited increased sensitivity to MV as compared to wild type. Interestingly expression of the RCD1$^{S/T}$IDR2^{A} form in *rcd1* led to only partial complementation of *rcd1* MV tolerance. This suggests that phosphorylation of IDR2 is implicated not only in RCD1 turnover alone or in complex with transcription factors but also in its function as transcriptional co-regulator.

Phosphorylation of proteins by PPKs has been connected to protein stability earlier (Liu *et al*, 2017; Ni *et al*, 2017; Chen *et al*, 2018). Ni *et al* (2017) described that PPKs phosphorylated the phyB-PIF3 complex upon light exposure, thereby targeting it for degradation - with an additional unknown factor X involved in the process. Intriguingly, RCD1 interacts with several PIFs, including PIF3 (Jaspers *et al*, 2009), which also localize to NBs (Favero, 2020). Moreover, PIF3 has been connected to retrograde signaling from the chloroplast (Martin *et al.*, 2016), a process where RCD1 also plays a role (Shapiguzov *et al*, 2019). The data presented here reveal a mechanism by which RCD1 levels could be regulated *via* phosphorylation and suggest that PPKs might be involved in the MV-induced decrease in RCD1 protein abundance shown in Shapiguzov *et al* (2019). This represents posttranslational control of a negative transcriptional co-regulator. Such regulation would allow PPKs to adjust the functions of RCD1 in response to environmental stimuli.

Conclusions

Our results unveil a complex function and posttranslational regulation of RCD1 (**Figure 6**). RCD1 is targeted by its bipartite N-terminal NLS sequence to the nucleus (#1 in Figure 6) where it interacts with various proteins, including PPKs (#2) and various transcription factors (#3), and accumulates in a PAR-dependent manner in NBs of unknown nature and composition (#4). Localization of RCD1 to NBs and binding of PAR (#4) are mediated by its WWE- and the PARP-like-domains. The C-terminal RST-domain interacts with transcription factors (#3 in Fig. 6; Jaspers *et al*, 2009, 2010; Bugge *et al*, 2018). The localization of PPKs to NBs is RCD1-dependent; otherwise the exact order of these events (##2, 3, and 4) is undetermined.

The ability of RCD1 to interact with a large number of transcription factors supports a function as a hub protein which integrates various developmental as well as environmental signals. PAR-dependent localization of RCD1 in NBs suggests that the recognition of PARylated proteins by RCD1 acts as "guidance system" to correctly position RCD1-protein-complexes along the chromatin or in specific sub-nuclear domains. Taken together, according to the data presented here, RCD1 represents the first described nuclear PAR-reader in plants. Therefore, our model proposes a new mechanism of fine-tuning transcriptional regulation, involving PAR and a PAR-reader RCD1.

MATERIALS AND METHODS

Plants, mutants and chemical treatments. *Arabidopsis thaliana* plants were grown on soil (peat: vermiculite = 1:1) under white luminescent light (220-250 µmol m^{-2} s^{-1}) at a 12-hour photoperiod and 22/18 °C. Seedlings were grown for 10 days on 1 x MS basal medium (Sigma) with 0.5 % Phytagel (Sigma). Arabidopsis *rcd1-4* mutant (GK-229D11) was used as a background for all complementation lines. The *ppk* triple mutants were kindly provided by Dr Dmitri Nusinow (Donald Danforth Plant Science Center, St. Louis) and have been described in Huang *et al*, (2016). Treatments with chemicals methyl viologen (MV, 0.1 or 1 µM, as indicated in the figures) and 3-methoxybenzamide (3MB, 10 mM) were performed on leaf discs floating on Milli-Q water supplemented with 0.05% Tween 20 (Sigma), overnight at room temperature or at 4˚C, accordingly.

Plasmids. Full-length AtRCD1, the WWE-domain (amino acids 1-155), RCD1ΔWWE (consisting of PARP- and RST-domains, amino acids 241-589) and the C-terminal part of RCD1 including the RST-domain (amino acids 468-589), were cloned into pGEX4T-1 for N-terminal GST fusion using primers listed in Supplementary table 3. Full-length AtRCD1 was also cloned into the pET8c vector for N-terminal His-fusion (Jaspers *et al*, 2010). For generating N-terminal GST-fusion constructs, PPK1-4 cDNAs were cloned into pGEX6P-1, and ASK cDNAs into pGEX4T-1. The kinase-dead ASK loss-of-function constructs contain a Lys-Arg mutation in the kinase activation loop.

For generating a GST fusion construct of RCD1 where the IDR2 is non-phosphorylateable (GST-RCD1$^{S/T}$IDR2^{A}), all phospho-serine and phospho-threonine residues within IDR2 were mutated to alanine residues by gene synthesis (Genescript Biotech, Netherlands).

To generate the RCD1-Venus construct, RCD1 cDNA was fused to the *UBIQUITIN10* promoter region and to the C-terminal triple Venus YFP tag in a MultiSite Gateway reaction as described in Siligato *et al*, (2016). The ΔWWE (missing the residues 90-151), ΔPARP (missing the residues 304-443) and ΔRST (missing the residues 462-589) deletions were introduced by PCR using primers listed in Supplementary table 3 and end-joining using In-Fusion (Clontech).

Construction of transgenic lines expressing HA-tagged RCD1 (RCD1-3xHA) is described in Jaspers *et al*, (2009). RCD1*nls*-HA variant was made using the vector pDONR/Zeo that contained the RCD1 promoter followed by the wild-type genomic RCD1 sequence (Jaspers *et al*, 2009). PCR was performed with Q5 High-Fidelity DNA Polymerase (New England Biolabs) and the primers listed in the Supplementary table 3. After sequential mutation of the two parts of the bipartite NLS, the

construct was transferred to the Gateway pGWB13 binary vector and introduced into the plants as described in Jaspers *et al*, (2009).

For generating epitope-tagged PPK fusions, the coding sequences of the four *PPK* genes lacking their stop codons were cloned into NcoI/XhoI-digested pENTR4 using In-Fusion enzyme (Clontech). The *PPK* coding sequences were then recombined by Gateway® Clonase II reactions into pH7WGR2 (Karimi *et al*, 2002) or pGWB414 (Nakagawa *et al*, 2007) to create RFP and 3xHA-tagged variants, respectively.

Spectroscopic measurements of photosynthesis. Chlorophyll fluorescence was measured by MAXI Imaging PAM (Walz, Germany) essentially as described in Shapiguzov *et al*, (2019). PSII photoinhibition protocol consisted of repetitive 1-hour periods of blue actinic light (450 nm, 80 µmol m^{-2} s^{-1}) each followed by a 20-min dark adaptation, then F_0 and F_m measurement. PSII photochemical yield was calculated as $F_v/F_m = (F_m-F_o)/F_m$. The assays were performed in 96-well plates. In each assay leaf discs from at least 4 individual plants were analyzed. Each assay was reproduced at least three times.

SDS-PAGE and immunoblotting. For immunoblotting of total plant extracts, the plant material was frozen immediately after treatments in liquid nitrogen and ground. Total proteins were extracted in SDS extraction buffer (50 mM Tris, pH 7.8, 2 % SDS, 1 x protease inhibitor cocktail; P9599, Sigma), 2 mg/ mL NaF) for 20 min at 37˚C and centrifuged at 18 000 x g for 10 min. Supernatants were normalized for protein concentration and resolved by SDS-PAGE. After electrophoresis, proteins were electroblotted to PVDF membrane and probed with specific antibodies: αHA (Roche), αGFP (Milteny Biotech), αGST (Sigma), αPAR (Trevigen), αRCD1 (Shapiguzov *et al*, 2019), and αAOX1/2 (Agrisera AS04 054). The signal was visualized by ECL Prime chemiluminescence reagents (GE Healthcare).

Confocal microscopy. The subcellular localization of RCD1 in stable expression Arabidopsis line was analyzed by confocal microscopy with a Leica SP5 II HCS inverted microscope using a solid-state blue laser was used for visualizing YFP and chloroplast autofluorescence (detection with 521–587 and 636–674 nm range, respectively). For co-localization studies of RCD1-Venus and PPK-RFP fusion constructs, the binary plasmids were transformed into *A. tumefaciens* strain GV3101 pMP90. Proteins were transiently expressed in *N. benthamiana* leaves as described below for co-immunoprecipitation assays. YFP was excited using a 488 nm laser with a detection window of 519-556 nm and RFP was excited using a 561 nm laser with detection at 599-657 nm.

Protein expression and purification. Fusion proteins were expressed in *E.coli* BL21 (DE3) Codon Plus strain and purified using GSH- or Ni^{2+}- Sepharose beads (GE Heathcare) according to manufacturer instructions as described before (Jaspers *et al*, 2009; Jaspers *et al*, 2010). The N-terminal GST-tagged WWE-domain of RNF146 (amino acids 100-175) was expressed and purified as described in Zhang *et al*, (2011).

Poly(ADP-ribose) dot-blot assay. Purified His and GST fusion proteins or GST alone (500 ng) were blotted onto nitrocellulose membrane (BioRad). The nitrocellulose membrane was rinsed with TBS-T buffer (10 mM Tris-HCl at pH 7.4, 150 mM NaCl and 0.05 % Tween 20) three times. The membrane was incubated with 100 nM of purified PAR (Trevigen, 4336-100-01, 10 µM stock, polymer size 2-300 units) for 1 h at room temperature. After 5 washes with TBS-T and TBS-T containing 1 M NaCl, the membrane was blocked with 5 % milk followed by immunoblotting with mouse αPAR (Trevigen) or αGST (Sigma) antibody.

Surface plasmon resonance. Recombinant RCD1-His and GST-RCD1ΔWWE proteins were coupled to a Biacore CM5 sensor chip *via* amino-groups. PAR (625 nM) was profiled at a flow rate of 30 mL/min for 300 s, followed by 600 s flow of wash buffer (10 mM HEPES, pH 7.4, 150 mM NaCl, 3 mM EDTA, 0.05% Surfactant P20). Mono ADP-ribose and cyclic ADP-ribose were profiled at 1 mM concentration. After analysis in BiaEvalution (Biacore), the normalized resonance units were plotted over time with the assumption of one-to-one binding.

Transient protein expression and co-immunoprecipitation. Binary vectors harbouring RCD1-GFP or PPK-3xHA fusions were transformed into *A. tumefaciens* strain GV3101 pMP90. For expression, Agrobacteria were scraped from selective YEB plates and resuspended in infiltration medium (10 mM MES pH 5.6, 10 mM $MgCl_2$) and the OD_{600} was adjusted to 0.8. To suppress transgene silencing, Agrobacteria expressing the tomato bushy stunt virus 19K silencing suppressor were co-infiltrated. After adding acetosyringone to a final concentration of 100 µM and incubation for 2 h at room temperature, Agrobacteria were mixed in a ratio of 1:1:2 (19K) and infiltrated into *N. benthamiana* leaves. Infiltrated leaf tissue was harvested 72 h later and proteins were extracted by grinding leaf tissue in liquid nitrogen followed by resuspension in extraction buffer (50 mM Tris-HCl pH 7.5, 150 mM NaCl, 10 % Glycerol, 1 mM EDTA, 5 mM DTT, 1 x protease inhibitor cocktail [P9599, Sigma], 10 µM MG132) at a ratio of 2 mL / g FW. Protein extracts were centrifuged at 20 000 x g / 4 °C / 20 min and a fraction of the supernatant was saved as 'input' sample. 15 µL of αGFP-nanobody:Halo:His6

magnetic beads (Chen *et al*, 2018) were added to 1.5 mLof protein extract followed by incubation on a rotating wheel at 4 ˚C for 5 min. The beads were washed 3 times with 1 mL extraction buffer using a magnetic tube rack and then boiled in 80 µL SDS sample buffer to elute protein from the beads. For immunoblots, protein samples were separated by SDS-PAGE and electro-blotted onto PVDF membrane. Antibodies used were αGFP (210-PS-1GP, Amsbio) and αHA (11867423001, Sigma).

Kinase activity assays. *In vitro* kinase assays using recombinant proteins were performed in a total volume of 20 µL of kinase buffer (20 mM HEPES, pH 7.5, 15 mM $MgCl_2$, and 5 mM EGTA). The reaction was started with 2 µCi [γ-^{32}P]ATP and incubated at room temperature for 30 min. The reaction was stopped by the addition of 5 µL of 4x SDS loading buffer. Proteins were resolved by SDS-PAGE and the gel was dried and exposed overnight to a phosphor imager screen. For the kinase activity test, GST-PPKs were tested against 5 µg myelin basic protein (MBP; Sigma Aldrich) and 5 µg Casein in 0.1 M Tris pH 8.8 (Sigma). For identification of *in vitro* phosphorylation sites by LC-MS/MS, 1.5 mM unlabeled ATP was used in the kinase buffer. The proteins were separated by SDS-PAGE, followed by Coomassie Brilliant Blue staining and were digested by trypsin (Promega).

LC-MS/MS. Phosphopeptides were enriched from tryptic digests using TiO_2 microcolumns (GL Sciences Inc., Japan) as described in Larsen *et al*, (2005). Enriched phosphopeptides were analyzed by a Q Exactive mass spectrometer (Thermo Fisher Scientific) connected to Easy NanoLC 1000 (Thermo Fisher Scientific). Peptides were first loaded on a trapping column and subsequently separated inline on a 15-cm C18 column (75 µm × 15 cm, ReproSil-Pur 5 µm 200 Å C18-AQ, Dr. Maisch HPLC). The mobile phase consisted of water with 0.1% (v/v) formic acid (solvent A) or acetonitrile/water (80:20 [v/v]) with 0.1% (v/v) formic acid (solvent B). A linear 60-min gradient from 6 to 42% (v/v) B was used to elute peptides. Mass spectrometry data were acquired automatically by using Xcalibur 3.1 software (Thermo Fisher Scientific). An information-dependent acquisition method consisted of an Orbitrap mass spectrometry survey scan of mass range 300 to 2000 m/z (mass-to-charge ratio) followed by higher-energy collisional dissociation (HCD) fragmentation for 10 most intense peptide ions. Raw data were searched for protein identification by Proteome Discoverer (version 2.2) connected to in-house Mascot (v. 2.6.1) server. Phosphorylation site locations were validated using phosphoRS algorithm. A SwissProt database (https://www.uniprot.org/) with a taxonomy filter Arabidopsis. Two missed cleavages were allowed. Peptide mass tolerance ± 10 ppm and fragment mass tolerance ± 0.02 D were used. Carbamidomethyl (C) was set as a fixed modification and Met oxidation, acetylation of

protein N-terminus, and phosphorylation of Ser and Thr were included as variable modifications. Only peptides with a false discovery rate of 0.01 were used.

ACKNOWLEDGEMENTS

We thank Mr Damien Marchese and Dr. Melanie Carmody for the help in generating the transgenic lines. We thank Dr. Dmitri Nusinow for providing the seeds of *ppk* triple mutants. We thank Maria Aatonen and Maria Semenova for help in Biacore experiments which were performed at the Biomolecular Interaction Unit, Faculty of Biological and Environmental Sciences, University of Helsinki. We thank Mika Molin and Marko Crivaro for help with confocal microscopy at the Light Microscopy Unit of the Institute of Biotechnology, University of Helsinki. Mass spectrometry analyses were performed at the Turku Proteomics Facility, supported by Biocenter Finland. This work was supported by the University of Helsinki (JK); the Academy of Finland Centre of Excellence programs (2006-11; and 2014-19; JK) and Research Grant (Decision 250336; JK). MW acknowledges funding from the Academy of Finland (Decisions 275632, 283139, 312498, and 323917). LW acknowledges funding by the German Research Foundation (DFG; grant WI 3670/2-1) and core funding from the Leibniz Institute for Plant Biochemistry (IPB) and the FU Berlin Dahlem Centre of Plant Sciences.

AUTHOR CONTRIBUTION

JV, AS, JKW, RG, CJ, LW, MW, and JK conceived and designed experiments. JV, AS, JKW, RDM, RG, ID, NB, and LW carried out experiments. JV, AS, JKW, RDM, RG, ID, NB, CJ, LW, MW, and JK analyzed the data. JV, AS, JKW, LW, and JK wrote the article. All authors read and contributed to the final article.

519 REFERENCES

520 **Adams-Phillips L, Briggs AG, Bent AF. 2010.** Disruption of poly(ADP-ribosyl)ation mechanisms
521 alters responses of Arabidopsis to biotic stress. *Plant Physiology* **152**:267–280
522 **Ahel I, Ahel D, Matsusaka T, Clark AJ, Pines J, Boulton SJ, West SC. 2008.** Poly(ADP-ribose)-
523 binding zinc finger motifs in DNA repair/checkpoint proteins. *Nature* **451**:81–85.
524 **Ahlfors R, Lång S, Overmyer K, Jaspers P, Brosché M, Tauriainen A, Kollist H, Tuominen H,**
525 **Belles-Boix E, Piippo M *et al*. 2004.** Arabidopsis RADICAL-INDUCED CELL DEATH1 belongs to
526 the WWE protein-protein interaction domain protein family and modulates abscisic acid, ethylene, and
527 methyl jasmonate responses. *Plant Cell* **16**:1925-1937.
528 **Aravind L. 2001.** The WWE domain: a common interaction module in protein ubiquitination and ADP
529 ribosylation. *Trends in Biochemical Sciences* **26**:273-275.
530 **Babiychuk E, Cottrill PB, Storozhenko S, Fuangthong M, Chen Y, O'Farrell MK, Van Montagu**
531 **M, Inzé D, Kushnir S. 1998**. Higher plants possess two structurally different poly(ADP-ribose)
532 polymerases. *The Plant Journal* **15**:635-645.
533 **Bah A, Forman-Kay JD. 2016.** Modulation of intrinsically disordered protein function by post-
534 translational modifications. *Journal of Biological Chemistry* **291**:6696-6705.
535 **Briggs AG, Bent AF. 2011.** Poly(ADP-ribosyl)ation in plants. *Trends in Plant Science* **16**:372–380.
536 **Brosché M, Blomster T, Salojärvi J, Cui F, Sipari N, Leppälä J, Lamminmäki A, Tomai G,**
537 **Narayanasamy S, Reddy RA *et al*. 2014.** Transcriptomics and functional genomics of ROS-induced
538 cell death regulation by RADICAL-INDUCED CELL DEATH1. *PLoS Genetics* **10**:e1004112.
539 **Bugge K, Staby L, Kemplen KR, O'Shea C, Bendsen SK, Jensen MK, Olsen JG, Skriver K,**
540 **Kragelund BB. 2018.** Structure of Radical-Induced Cell Death1 hub domain reveals a common αα-
541 scaffold for disorder in transcriptional networks. *Structure* **26**:734-746.
542 **Chen C, Masi R, Lintermann R, Wirthmueller L. 2018.** Nuclear import of *Arabidopsis* poly(ADP-
543 ribose) polymerase 2 is mediated by importin-α and a nuclear localization sequence located between
544 the predicted SAP domains. *Frontiers in Plant Science* **9**:1581.
545 **Chen HH, Qu L, Xu ZH, Zhu JK, Xue HW. 2018.** EL1-like casein kinases suppress ABA signaling
546 and responses by phosphorylating and destabilizing the ABA receptors PYR/PYLs in *Arabidopsis*.
547 *Molecular Plant* **11**:706-719.

Christensen LF, Staby L, Bugge K, O'Shea C, Kragelund BB, Skriver K. 2019. Evolutionary conservation of the intrinsic disorder-based Radical-Induced Cell Death1 hub interactome. *Scientific Reports* **9**:18927.

Christians MJ, Gingerich DJ, Hua Z, Lauer TD, Vierstra RD. 2012. The light-response BTB1 and BTB2 proteins assemble nuclear ubiquitin ligases that modify phytochrome B and D signaling in Arabidopsis. *Plant Physiology* **160**:118-134.

Cohen MS, Chang P. 2018. Insights into the biogenesis, function, and regulation of ADP-ribosylation. *Nature Chemical Biology* **14**:236-243.

DaRosa PA, Wang Z, Jiang X, Pruneda JN, Cong F, Klevit RE, Xu W. 2015. Allosteric activation of the RNF146 ubiquitin ligase by a poly(ADP-ribosyl)ation signal. *Nature* **517**:223-226.

Favero DS. 2020. Mechanisms regulating PIF transcription factor activity at the protein level. *Physiologia Plantarum*. doi: 10.1111/ppl.13075.

Feng B, Liu C, de Oliveira MV, Intorne AC, Li B, Babilonia K, de Souza Filho GA, Shan L, He P. 2015. Protein poly(ADP-ribosyl)ation regulates *Arabidopsis* immune gene expression and defense responses. *PLoS Genetics* **11**:e1004936

Feng B, Ma S, Chen S, Zhu N, Zhang S, Yu B, Yu Y, Le B, Chen X, Dinesh-Kumar SP et al. 2016. PARylation of the Forkhead-associated domain protein DAWDLE regulates plant immunity. *EMBO Reports* **17**:1799-1813.

Fujibe T, Saji H, Arakawa K, Yabe N, Takeuchi Y, Yamamoto KT. 2004. A methyl viologen-resistant mutant of Arabidopsis, which is allelic to ozone-sensitive *rcd1*, is tolerant to supplemental ultraviolet-B irradiation. *Plant Physiology* **134**:275-285.

Gupte R, Liu Z, Kraus WL. 2017. PARPs and ADP-ribosylation: recent advances linking molecular functions to biological outcomes. *Genes & Development* **31**:101-126.

Hiltscher H, Rudnik R, Shaikhali J, Heiber I, Mellenthin M, Meirelles Duarte I, Schuster G, Kahmann U, Baier M. 2014. The radical induced cell death protein 1 (RCD1) supports transcriptional activation of genes for chloroplast antioxidant enzymes. *Frontiers in Plant Science* **5**:475.

Huang H, Alvarez S, Bindbeutel R, Shen Z, Naldrett MJ, Evans BS, Briggs SP, Hicks LM, Kay SA, Nusinow DA. 2016. Identification of Evening complex associated proteins in *Arabidopsis* by affinity purification and mass spectrometry. *Molecular and Cellular Proteomics* **15**:201-217.

Iakoucheva LM, Radivojac P, Brown CJ, O'Connor TR, Sikes JG, Obradovic Z, Dunker AK. 2004. The importance of intrinsic disorder for protein phosphorylation. *Nucleic Acids Research* **32**:1037-1049.

Jaspers P, Blomster T, Brosché M, Salojärvi J, Ahlfors R, Vainonen JP, Reddy RA, Immink R, Angenent G, Turck F *et al*. 2009. Unequally redundant RCD1 and SRO1 mediate stress and developmental responses and interact with transcription factors. *The Plant Journal* **60**:268-279.

Jaspers P, Overmyer K, Wrzaczek M, Vainonen JP, Blomster T, Salojärvi J, Reddy RA, Kangasjärvi J. 2010. The RST and PARP-like domain containing SRO protein family: analysis of protein structure, function and conservation in land plants. *BMC Genomics* **11**:170.

Jespersen N, Barbar E. 2020. Emerging Features of Linear Motif-Binding Hub Proteins. *Trends in Biochemical Sciences* **45**:375-384.

Jungmichel S, Rosenthal F, Altmeyer M, Lukas J, Hottiger MO, Nielsen ML. 2013. Proteome-wide identification of poly(ADP-Ribosyl)ation targets in different genotoxic stress responses. *Molecular Cell* **52**:272–285.

Karimi M, Inzé D, Depicker A. 2002. GATEWAY vectors for *Agrobacterium*-mediated plant transformation. *Trends in Plant Science* **7**:193-195.

Kim DS, Challa S, Jones A, Kraus WL. 2020. PARPs and ADP-ribosylation in RNA biology: from RNA expression and processing to protein translation and proteostasis. *Genes & Development* **34**:302-320.

Kragelund BB, Jensen MK, Skriver K. 2012. Order by disorder in plant signaling. *Trends in Plant Science* **17**:625-32.

Lamb RS, Citarelli M, Teotia S. 2012. Functions of the poly(ADP-ribose) polymerase superfamily in plants. *Cellular and Molecular Life Sciences* **69**:175–189.

Leung AKL. 2017. PARPs. *Current Biology* **27**:R1256-R1258.

Liu Q, Wang Q, Deng W, Wang X, Piao M, Cai D, Li Y, Barshop WD, Yu X, Zhou T *et al*. 2017. Molecular basis for blue light-dependent phosphorylation of *Arabidopsis* cryptochrome 2. *Nature Communications* **8**:15234.

Love AJ, Yu C, Petukhova NV, Kalinina NO, Chen J, Taliansky ME. 2017. Cajal bodies and their role in plant stress and disease responses. *RNA Biology* **14**:779-790.

Mao YS, Zhang B, Spector DL. 2011. Biogenesis and function of nuclear bodies. *Trends in Genetics* **27**:295-306.

608 **Martello R, Leutert M, Jungmichel S, Bilan V, Larsen SC, Young C, Hottiger MO, Nielsen ML.**
609 **2016.** Proteome-wide identification of the endogenous ADP-ribosylome of mammalian cells and tissue.
610 *Nature Communications* **7**:12917.
611 **Martín G, Leivar P, Ludevid D, Tepperman JM, Quail PH, Monte E. 2016**. Phytochrome and
612 Retrograde Signalling Pathways Converge to Antagonistically Regulate a Light-Induced
613 Transcriptional Network. *Nature Communications* **7**:11431.
614 **McLellan H, Boevink PC, Armstrong MR, Pritchard L, Gomez S, Morales J, Whisson SC,**
615 **Beynon JL, Birch PR. 2013.** An RxLR effector from *Phytophthora infestans* prevents re-localisation
616 of two plant NAC transcription factors from the endoplasmic reticulum to the nucleus. *PLoS Pathogens*
617 **9**:e1003670.
618 **Mergner J, Frejno M, List M, Papacek M, Chen X, Chaudhary A, Samaras P, Richter S, Shikata**
619 **H, Messerer M *et al*. 2020**. Mass-spectrometry-based draft of the *Arabidopsis* proteome. *Nature*
620 579:409-414.
621 **Nakagawa T, Suzuki T, Murata S, Nakamura S, Hino T, Maeo K, Tabata R, Kawai T, Tanaka K,**
622 **Niwa Y *et al*. 2007.** Improved Gateway binary vectors: high-performance vectors for creation of fusion
623 constructs in transgenic analysis of plants. *Bioscience Biotechnology, and Biochemistry* **71**: 2095-2100.
624 **Ni W, Xu SL, Gonzalez-Grandio E, Chalkley RJ, Huhmer AFR, Burlingame AL, Wang ZY,**
625 **Quail PH**. **2017.** PPKs mediate direct signal transfer from phytochrome photoreceptors to
626 transcription factor PIF3. *Nature Communications* **8**:15236.
627 **O'Shea C, Staby L, Bendsen SK, Tidemand FG, Redsted A, Willemoës M, Kragelund BB,**
628 **Skriver K. 2017.** Structures and short linear motif of disordered transcription factor regions provide
629 clues to the interactome of the cellular hub protein Radical-induced Cell Death1. *Journal of Biological*
630 *Chemistry* **292**:512-527.
631 **Overmyer K, Tuominen H, Kettunen R, Betz C, Langebartels C, Sandermann H Jr, Kangasjärvi**
632 **J. 2000**. Ozone-sensitive Arabidopsis *rcd1* mutant reveals opposite roles for ethylene and jasmonate
633 signaling pathways in regulating superoxide-dependent cell death. *Plant Cell* **12**:1849-1862.
634 **Palazzo L, Leidecker O, Prokhorova E, Dauben H, Matic I, Ahel I. 2018.** Serine is the major
635 residue for ADP-ribosylation upon DNA damage. *Elife* **7**: e34334.
636 **Qin F, Sakuma Y, Tran LS, Maruyama K, Kidokoro S, Fujita Y, Fujita M, Umezawa T, Sawano**
637 **Y, Miyazono K *et al*. 2008**. *Arabidopsis* DREB2A-interacting proteins function as RING E3 ligases
638 and negatively regulate plant drought stress-responsive gene expression. *Plant Cell* **20**, 1693–1707.

Reddy AS, Day IS, Göhring J, Barta A. 2012. Localization and dynamics of nuclear speckles in plants. *Plant Physiology* **158**:67-77.

Saidi Y, Hearn TJ, Coates JC. 2012. Function and evolution of 'green' GSK3/Shaggy-like kinases. *Trends in Plant Science* **17**:39-46.

Shapiguzov A, Vainonen JP, Hunter K, Tossavainen H, Tiwari A, Järvi S, Hellman M, Aarabi F, Alseekh S, Wybouw B *et al*. 2019. Arabidopsis RCD1 coordinates chloroplast and mitochondrial functions through interaction with ANAC transcription factors. *Elife* **8**: e43284.

Siligato R, Wang X, Yadav SR, Lehesranta S, Ma G, Ursache R, Sevilem I, Zhang J, Gorte M, Prasad K *et al*. 2016. MultiSite Gateway-compatible cell type-specific gene-inducible system for plants. *Plant Physiology* **170**: 627-641.

Simon L, Voisin M, Tatout C, Probst AV. 2015. Structure and function of centromeric and pericentromeric heterochromatin in *Arabidopsis thaliana*. *Frontiers in Plant Science* **6**:1049.

Song J, Keppler BD, Wise RR, Bent AF. **2015.** PARP2 Is the predominant poly(ADP-Ribose) polymerase in Arabidopsis DNA damage and immune responses. *PLoS Genetics* **11**:e1005200.

Stampfl H, Fritz M, Dal Santo S, Jonak C. 2016. The GSK3/Shaggy-Like Kinase ASKα Contributes to Pattern-Triggered Immunity. *Plant Physiology* **171**:1366-1377.

Su Y, Wang S, Zhang F, Zheng H, Liu Y, Huang T, Ding Y. 2017. Phosphorylation of histone H2A at Serine 95: a plant-specific mark involved in flowering time regulation and H2A.Z deposition. *Plant Cell* **29**:2197-2213.

Teloni F, Altmeyer M. 2016. Readers of poly(ADP-ribose): designed to be fit for purpose. *Nucleic Acids Research* **44**:993-1006.

Teotia S, Lamb RS. 2009. The paralogous genes *RADICAL-INDUCED CELL DEATH1* and *SIMILAR TO RCD ONE1* have partially redundant functions during Arabidopsis development. *Plant Physiology* **151**:180-198.

Vainonen JP, Jaspers P, Wrzaczek M, Lamminmäki A, Reddy RA, Vaahtera L, Brosché M, Kangasjärvi J. 2012. RCD1-DREB2A interaction in leaf senescence and stress responses in *Arabidopsis thaliana*. *Biochemical Journal* **442**:573-581.

Vainonen JP, Shapiguzov A, Vaattovaara A, Kangasjärvi J. 2016. Plant PARPs, PARGs and PARP-like proteins. *Current Protein and Peptide Science* **17**:713-723.

Van Buskirk EK, Decker PV, Chen M. 2012. Photobodies in light signaling. *Plant Physiology* **158**:52-60.

Wang Z, Michaud GA, Cheng Z, Zhang Y, Hinds TR, Fan E, Cong F, Xu W. 2012. Recognition of the iso-ADP-ribose moiety in poly(ADP-ribose) by WWE domains suggests a general mechanism for poly(ADP-ribosyl)ation-dependent ubiquitination. *Genes & Development* **26**:235-240.

Wang Z, Casas-Mollano JA, Xu J, Riethoven JJ, Zhang C, Cerutti H. 2015. Osmotic stress induces phosphorylation of histone H3 at threonine 3 in pericentromeric regions of *Arabidopsis thaliana*. *Proceedings of the National Academy of Sciences, USA* **112**:8487-8492.

Wirthmueller L, Asai S, Rallapalli G, Sklenar J, Fabro G, Kim DS, Lintermann R, Jaspers P, Wrzaczek M, Kangasjärvi J *et al*. 2018. *Arabidopsis* downy mildew effector HaRxL106 suppresses plant immunity by binding to RADICAL-INDUCED CELL DEATH1. *New Phytologist* **220**:232-248.

Zhang Y, Liu S, Mickanin C, Feng Y, Charlat O, Michaud GA, Schirle M, Shi X, Hild M, Bauer A *et al*. 2011. RNF146 is a poly(ADP-ribose)-directed E3 ligase that regulates axin degradation and Wnt signalling. *Nature Cell Biology* **13**:623-629.

Zhang YJ, Wang JQ, Ding M, Yu YH. **2013.** Site-specific characterization of the Asp- and Glu-ADP-ribosylated proteome. *Nature Methods* **10**:981–984.

Zheng H, Zhang F, Wang S, Su Y, Ji X, Jiang P, Chen R, Hou S, Ding Y. 2018. MLK1 and MLK2 coordinate RGA and CCA1 to regulate hypocotyl elongation in *Arabidopsis thaliana*. *Plant Cell* **30**:67-82.

Table 1: List of phosphosites identified *in vivo* or after *in vitro* kinase assay using PPKs.

Phosphopeptide	**Contained phosphosites**	**Study**
VLDssRCEDGFGK	S11, S12	*in vitro* PPK (a)
AAsYAAYVtGVsCAK	S27, T33, S36	*in vivo* (b), *in vitro* PPK (a)
LEIDVNGGEtPR	T204	*in vivo* (a, b)
LNLEECsDEsGDNMMDDVPLAQR	S213, S216	*in vitro* PPK (a)
ssNEHYDEAtEDCsR	S230, S231, T239, S242, S244	*in vivo* (b), *in vitro* PPK (a)
KLEAAVsK	S252	*in vivo* (a), *in vitro* PPK (a)
WDEtDAIVVsGAK	T257, S263	*in vivo* (b)
LTGsEVLDK	S270	*in vitro* PPK (a)
FssEIAEAR	S301, S302	*in vitro* PPK (a)
QVEItKK	T319	*in vitro* PPK (a)
DNsGVtLEGPK	S467, T470	*in vivo* (a), *in vitro* PPK (a)
GsGsANsVGssttRPK	S490, S492, S495, S498, S499, T500, T501	*in vivo* (a), *in vitro* PPK (a)
EIPGsIR	S578	*in vitro* PPK (a)

(a) this study, (b) Wirthmueller *et al*, 2018. Phosphopeptides between the WWE- and PARP-like-domains are marked with *italic*. Lowercase s and t represent phosphorylated serine and threonine residues respectively. The full list of phosphopeptides identified in this study is present in Supplementary table 2.

FIGURE LEGENDS

Figure 1. Nuclear localization of RCD1 is essential for its function.

A. Schematic representation of RCD1 domain structure containing a bipartite NLS, WWE-, PARP-like- and RST-domains. Intrinsically disordered regions between the domains are marked as IDR1-4.

B. *rcd1*-specific curly leaf phenotype in RCD1*nls*-HA lines. *rcd1* phenotype can be complemented by re-introduction of wild type RCD1-HA into the mutant background, but not by RCD1 with mutated NLS. Picture shows 5-week-old plant rosettes of two independent lines (A and B) for each construct under standard growth conditions.

C. RCD1 requires its NLS to complement the *rcd1*-specific MV tolerance. PSII inhibition (Fv/Fm) by methyl viologen (MV) was measured in indicated lines using 1 μM MV. For each experiment, leaf discs from three individual rosettes were used. The experiment was performed three times with similar results. Mean ± SD are shown. *** – P-value < 0.001 with Bonferroni corrected *post hoc* test; n.s. – non-significant difference. Source data and statistics are presented in Supplementary table 1.

D. Disruption of NLS leads to higher RCD1 accumulation in plants. Abundance of RCD1-HA in indicated RCD1*nls*-HA and RCD1-HA lines was assessed by immunoblot analysis with HA-specific antibodies. A total protein amount of 100 μg corresponds to 100%. Rubisco large subunit detected by amido black staining is shown as a control for protein loading.

Figure 2. RCD1 localizes to NBs dependent on WWE- and PARP-like-domains and binds PAR.

A. Deletion of the WWE- or PARP-like-domains, but not the RST-domain, prevents NB localization of RCD1. Confocal images were taken from stable Arabidopsis lines expressing full-length RCD1-Venus, RCD1ΔWWE-Venus, RCD1ΔPARP-Venus or RCD1ΔRST-Venus.

B. NB formation by RCD1 is diminished by a PARP inhibitor 3MB. Plants expressing RCD1-Venus were pretreated overnight at 4°C without (control) or with 3MB, after which confocal images were taken.

C. RCD1 binds PAR *in vitro*. PAR binding activity of immobilized GST-tagged domains of RCD1 and full-length RCD1-His was assessed by dot-blot assay using PAR-specific antibody. GST tagged human WWE-domain (hWWE) and GST were used as positive and negative controls, respectively. GST antibody was used to assess protein loading.

D. WWE domain of RCD1 is required for interaction with PAR. SPR sensorgrams of interaction between immobilized RCD1-His or GST-RCD1ΔWWE and PAR profiled at 625 nM. Increase in response units shows association of PAR with RCD1-His but not with GST-RCD1ΔWWE**.**

Figure 3. PPK localization to NBs is RCD1-dependent.

A. RCD1 colocalizes with PPKs in NBs in tobacco. RCD1-Venus was co-expressed with RFP or RFP-tagged PPKs in epidermal cells of *N. benthamiana* and the subnuclear localization was analyzed by confocal microscopy.

B. PPK-RFPs alone do not form NB. PPK-RFP fusion proteins were expressed as in (A) but without co-expression of RCD1-Venus.

Figure 4. PPKs phosphorylate RCD1 at multiple sites.

A. Representation of RCD1 phosphosites identified by *in vivo* and *in vitro* analyses. RCD1 domains are highlighted in blue and named on top of the sequence. Individual phosphosites are marked in red and numbered.

B, C. Phosphosites in the region between WWE- and PARP-like-domains are targets for PPKs. Recombinant GST-PPK2 and GST-PPK4 were used together with recombinant GST-RCD1 protein in *in vitro* kinase assays. GST-PPK2 and 4 (asterisks) showed activity towards GST-RCD1 (red arrowhead). There was no activity detected against the mutated GST-RCD1$^{S/T}$IDR2^{A} protein. Upper panel shows autoradiograph, lower panel shows the Coomassie-stained SDS-PAGE.

D. Phosphorylation of IDR2 of RCD1 by PPKs affects its stability and function. *In vivo* abundance of RCD1$^{S/T}$IDR2^{A}-HA and of wild-type RCD1-HA variants was assessed in independent transgenic lines by immunoblot analysis with HA-specific antibody. The RCD1$^{S/T}$IDR2^{A}-HA variant did not fully complement *rcd1*-specific accumulation of alternative oxidases (AOX1/2), as revealed by immunoblot with αAOX1/2 antibodies. Rubisco large subunit detected by amido black staining is shown as a control for equal protein loading.

E. RCD1$^{S/T}$IDR2^{A}-HA variant does not fully complement *rcd1*-specific tolerance to MV. PSII inhibition (Fv/Fm) by MV was measured in indicated lines using 1 μM MV. For each experiment, leaf discs from at least four individual rosettes were used. The experiment was performed three times with similar results. Mean ± SD are shown. *** – P-value < 0.001 with Bonferroni corrected *post hoc* test at

the selected time points between *rcd1*: RCD1$^{S/T}$IDR2^{A}-HA (line B) and *rcd1*: RCD1-HA lines. Full source data and statistics are presented in Supplementary table 1.

Figure 5. Knockout of PPKs stabilizes native RCD1.

A. RCD1 accumulation in *ppk* triple mutants is higher than in Col-0. RCD1 level was assessed in total protein extracts from 3-week-old plants by immunoblot analysis with RCD1-specific antibody. Rubisco large subunit detected by amido black staining is shown as a control for equal protein loading.

B. *ppk* triple mutants are more sensitive to MV than Col-0. PSII inhibition (Fv/Fm) by MV was measured in indicated lines using 0.1 μM MV. For each experiment, leaf discs from four individual rosettes were used. The experiment was performed three times with similar results. Mean ± SD are shown. * – P-value < 0.05 with Bonferroni corrected *post hoc* test at the selected time point between *ppk124* and Col-0. Source data and statistics are presented in Supplementary table 1.

Figure 6. A model describing the regulation of nuclear RCD1 function in dependence of PAR binding and phosphorylation by PPKs. (1) RCD1 enters the nucleus by means of its bipartite N-terminal NLS sequence. In the nucleus, RCD1 interacts with PPKs (2), with diverse transcription factors (3) and with PAR (4). PAR recruits RCD1 to NBs of yet uncharacterized nature. Unknown PARylated proteins involved in RCD1 recruitment are labeled with a question mark. RCD1 is phosphorylated by PPKs at multiple sites in IDR2 (5), which targets RCD1 for degradation (6). RCD1 structure was predicted in RaptorX (http://raptorx.uchicago.edu/). Structural model of the WWE-domain is based on mouse RNF146 (2RSF), structures of RCD1 PARP-like- (5NGO, Wirthmueller *et al*, 2018) and RST- (5N9Q, Bugge *et al*, 2018) domains have been reported. Terminal and inter-domain regions of RCD1 are not drawn to scale.

Supplementary information.

Supplementary figure 1. Characterization of stable transgenic lines expressing RCD1 domain deletion constructs fused to triple Venus tag in *rcd1* background.

A. Schematic representation of domain deletion constructs in complementation lines.

B. Expression of RCD1 domain deletion constructs in *rcd1* background complements *rcd1*-specific curly leaf phenotype. Pictures show 5-week-old plant rosettes of two independent lines (A and B) for each construct under standard growth conditions.

C. MV sensitivity is restored in lines expressing RCD1-Venus, RCD1ΔWWE-Venus and RCD1ΔPARP-Venus constructs, but only partially in lines expressing RCD1ΔRST-Venus. PSII inhibition (Fv/Fm) by MV was measured in indicated lines using 1 μM MV. For each experiment, leaf discs from three individual rosettes were used. The experiment was performed three times with similar results. Mean ± SD are shown. *** – P-value < 0.001 with Bonferroni corrected *post hoc* test. Source data and statistics are presented in Supplementary table 1.

D. Domain deletion does not lead to decreased expression of RCD1. RCD1 level in indicated lines was assessed by immunoblot analysis of total protein extracts with GFP-specific antibody. A total amount of 100 μg protein was loaded.

Supplementary figure 2. RCD1 binds PAR but not ADP-ribose or cyclic ADP-ribose.

A. The purity of recombinant proteins used in *in vitro* analyses of PAR binding. Proteins were purified, resolved by SDS-PAGE and stained with Coomassie.

B, C. RCD1-His neither binds mono-ADP-ribose (ADPR), nor cyclic ADP-ribose (cADPR). SPR sensorgrams do not show any response in case of ADPR or cADPR profiled at 1 mM concentrations over immobilized RCD1-His.

D. PAR titration curve obtained by SPR analysis of PAR binding by RCD1-His. The curve was plotted using non-linear regression with the assumption of one-to-one binding.

Supplementary figure 3. RCD1 is phosphorylated *in-vivo*. RCD1-HA migrates in SDS-PAGE as a double band visualized by immunoblot analysis of protein extracts with HA-specific antibody. Upper band corresponding to phosphorylated form of RCD1-HA was diminished by treatment of plant extracts with alkaline phosphatase (CIP). Rubisco large subunit detected by amido black staining is shown as a control for equal protein loading.

Supplementary figure 4. **RCD1-GFP interacts with PPK-HA in tobacco.** RCD1-GFP was transiently co-expressed with HA-tagged versions of PPK1, 2, 3 or 4 in *N. benthamiana*. YFP served as negative control. At 72 hours post infiltration, RCD1-GFP and YFP were immunoprecipitated with GFP-specific antibody and co-precipitating PPK-HA proteins were detected by α-HA immunoblot. Immunoprecipitation of RCD1-GFP and YFP was confirmed by an α-GFP immunoblot. 'Input' samples were taken before immunoprecipitation and included on the immunoblots to test for equal expression and loading.

Supplementary figure 5. Recombinant PPK2 and PPK4 are active in *in vitro* kinase assays. Recombinant GST-PPK1-4 were used together with generic substrates casein and myelin basic protein (MBP) in an *in vitro* kinase assay. Upper panel shows autoradiograph, lower panel shows the Coomassie-stained SDS-PAGE.

Supplementary figure 6. ***In vivo* phosphorylation pattern of RCD1$^{S/T}$IDR2^{A}-HA is different from that of the wild type RCD1-HA.** Upper band corresponding to phosphorylated form of RCD1 is less abundant in RCD1$^{S/T}$IDR2^{A}-HA line as visualized by immunoblot analysis of protein extracts with HA-specific antibody. Lines A and B were chosen due to approximately equal expression of RCD1 in these lines (Figure 4D). 100% corresponds to 100 µg of total protein. Rubisco large subunit detected by amido black staining is shown as a control for equal protein loading.

Supplementary figure 7. ASKα, ASKγ, and ASKε phosphorylate RCD1 *in vitro*.
A. Specificity of ASKα, ASKγ and ASKε towards RCD1. Recombinant ASK-GSTs were used together with recombinant GST-RCD1 protein in an *in vitro* kinase assay.
B. Thr204 is the target for ASKs. ASKα,γ,ε -GST were used with recombinant GST-RCD1 or GST-RCD1T204A in an *in vitro* kinase assay. LOF indicates loss-of-function constructs of ASKs.
Upper panels shows autoradiographs, lower panels shows the Coomassie-stained SDS-PAGE.

Supplementary table 1. Source data and statistical analyses.

Supplementary table 2. Identified RCD1 phosphopeptides.

839

840 **Supplementary table 3**. Primers used in the study.

841

842

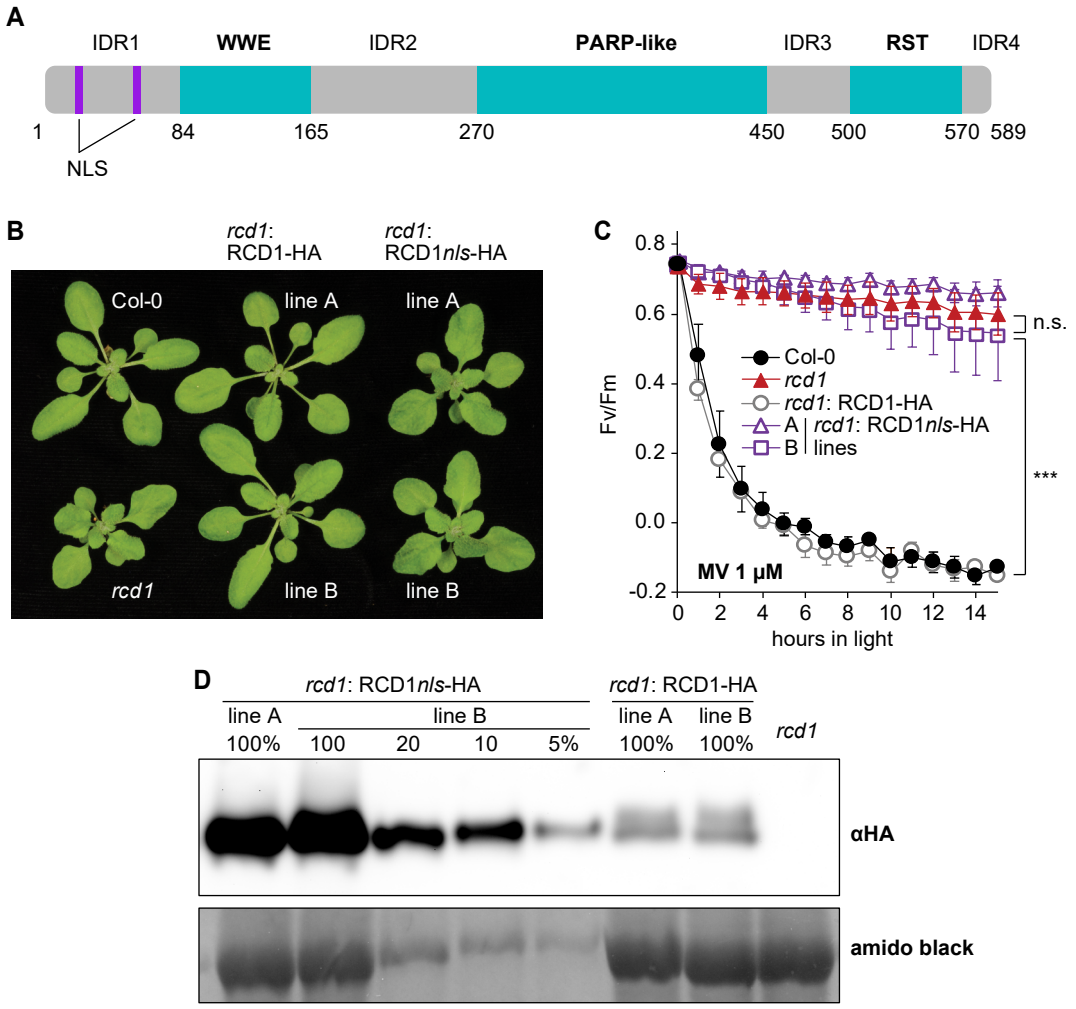

Figure 1. Nuclear localization of RCD1 is essential for its function.

A. Schematic representation of RCD1 domain structure containing a bipartite NLS, WWE-, PARP-like- and RST-domains. Intrinsically disordered regions between the domains are marked as IDR1-4.

B. *rcd1*-specific curly leaf phenotype in RCD1nls-HA lines. *rcd1* phenotype can be complemented by re-introduction of wild type RCD1-HA into the mutant background, but not by RCD1 with mutated NLS. Picture shows 5-week-old plant rosettes of two independent lines (A and B) for each construct under standard growth conditions.

C. RCD1 requires its NLS to complement the *rcd1*-specific MV tolerance. PSII inhibition (Fv/Fm) by methyl viologen (MV) was measured in indicated lines using 1 µM MV. For each experiment, leaf discs from three individual rosettes were used. The experiment was performed three times with similar results. Mean ± SD are shown. *** – P-value < 0.001 with Bonferroni corrected *post hoc* test; n.s. – non-significant difference. Source data and statistics are presented in Supplementary table 1.

D. Disruption of NLS leads to higher RCD1 accumulation in plants. Abundance of RCD1-HA in indicated RCD1*nls*-HA and RCD1-HA lines was assessed by immunoblot analysis with HA-specific antibodies. A total protein amount of 100 µg corresponds to 100%. Rubisco large subunit detected by amido black staining is shown as a control for protein loading.

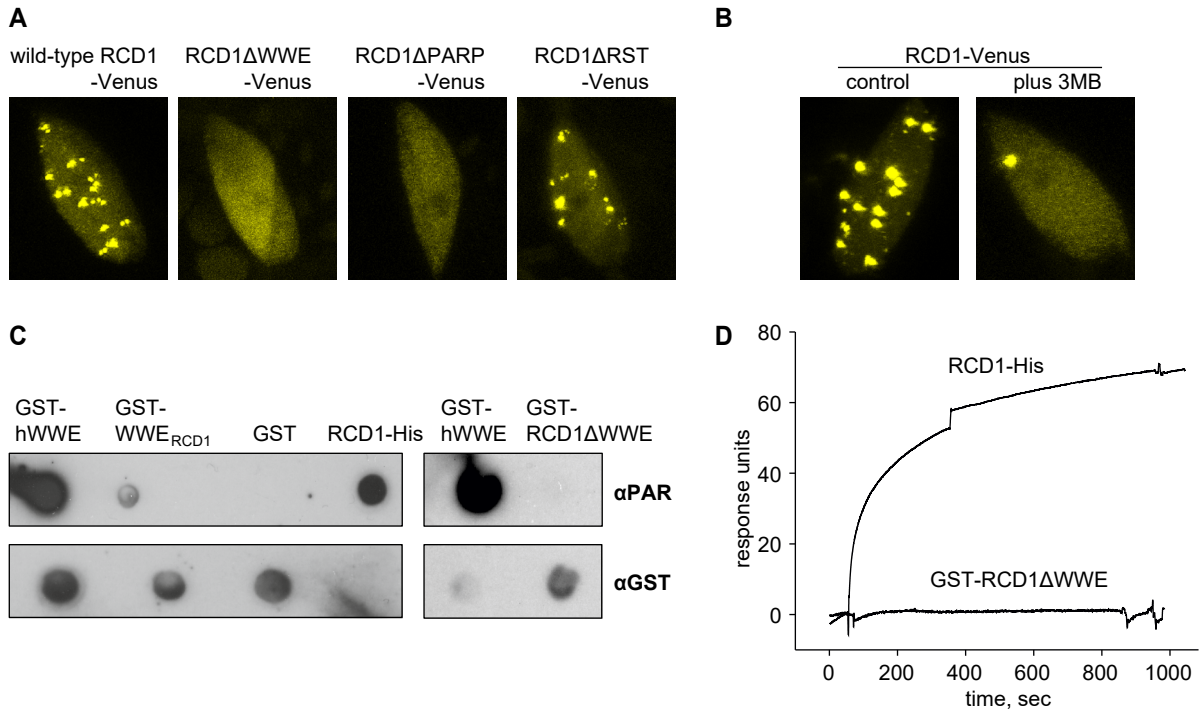

Figure 2. RCD1 localizes to NBs dependent on WWE- and PARP-like-domains and binds PAR.
A. Deletion of the WWE- or PARP-like-domains, but not the RST-domain, prevents NB localization of RCD1. Confocal images were taken from stable Arabidopsis lines expressing full-length RCD1-Venus, RCD1ΔWWE-Venus, RCD1ΔPARP-Venus or RCD1ΔRST-Venus.
B. NB formation by RCD1 is diminished by a PARP inhibitor 3MB. Plants expressing RCD1-Venus were pretreated overnight at 4°C without (control) or with 3MB, after which confocal images were taken.
C. RCD1 binds PAR *in vitro*. PAR binding activity of immobilized GST-tagged domains of RCD1 and full-length RCD1-His was assessed by dot-blot assay using PAR-specific antibody. GST tagged human WWE-domain (hWWE) and GST were used as positive and negative controls, respectively. GST antibody was used to assess protein loading.
D. WWE domain of RCD1 is required for interaction with PAR. SPR sensorgrams of interaction between immobilized RCD1-His or GST-RCD1ΔWWE and PAR profiled at 625 nM. Increase in response units shows association of PAR with RCD1-His but not with GST-RCD1ΔWWE.

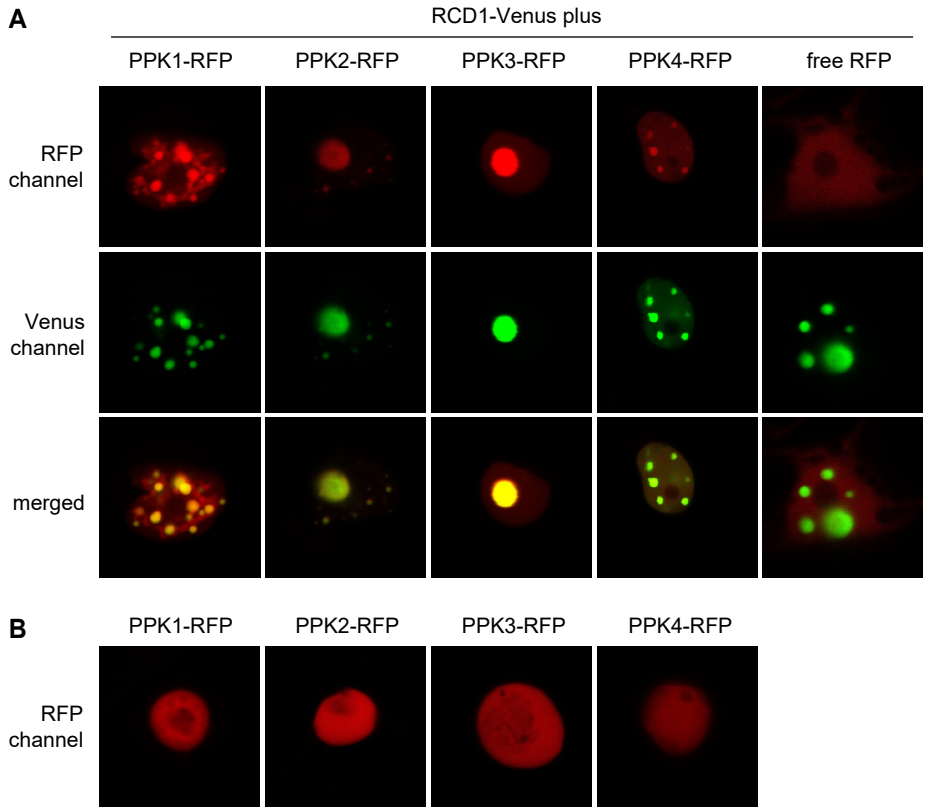

Figure 3. PPK localization to NBs is RCD1-dependent.

A. RCD1 colocalizes with PPKs in NBs in tobacco. RCD1-Venus was co-expressed with RFP or RFP-tagged PPKs in epidermal cells of *N. benthamiana* and the subnuclear localization was analyzed by confocal microscopy.

B. PPK-RFPs alone do not form NB. PPK-RFP fusion proteins were expressed as in (A) but without co-expression of RCD1-Venus.

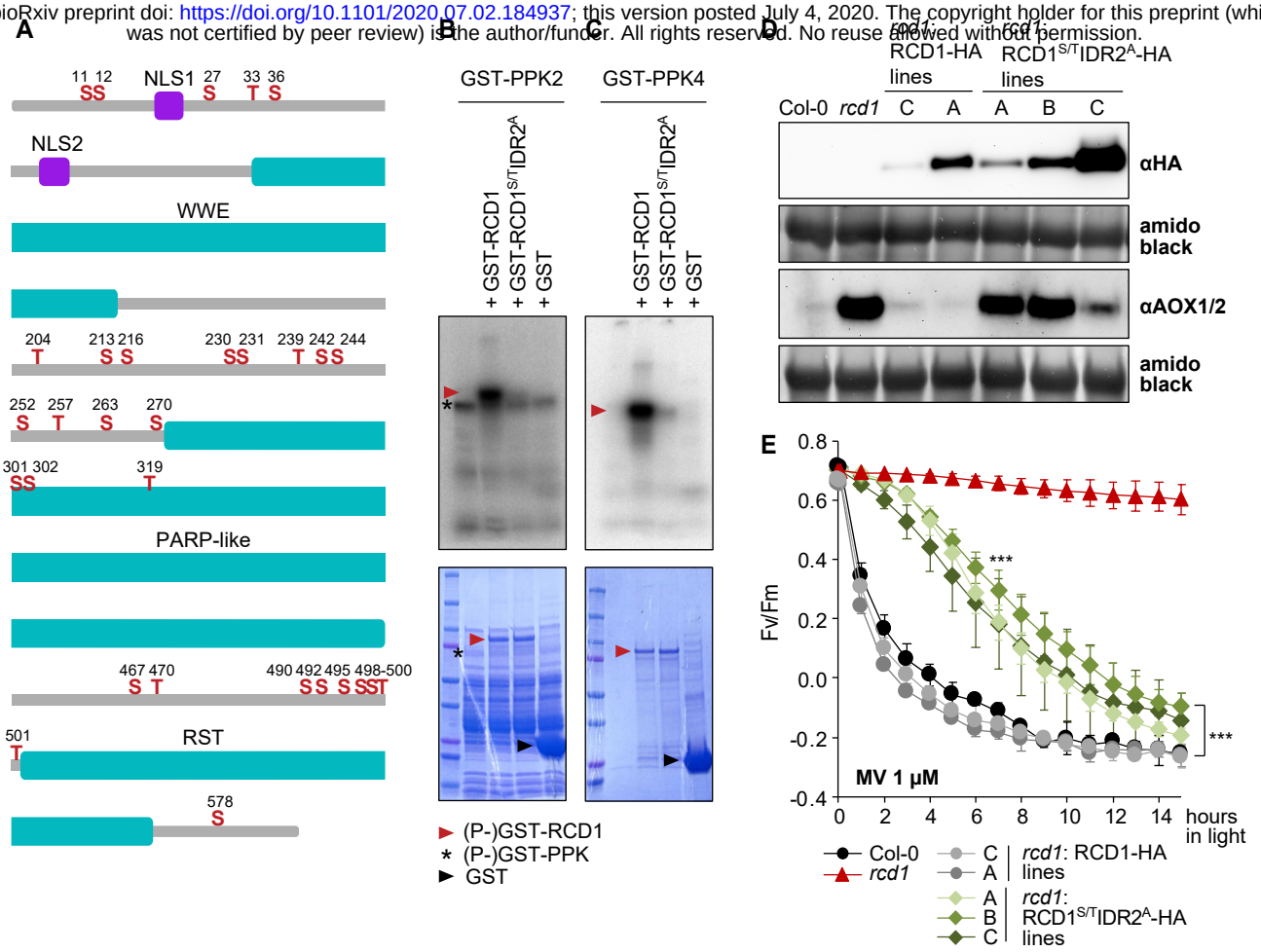

Figure 4. PPKs phosphorylate RCD1 at multiple sites.

A. Representation of RCD1 phosphosites identified by *in vivo* and *in vitro* analyses. RCD1 domains are highlighted in blue and named on top of the sequence. Individual phosphosites are marked in red and numbered.

B, C. Phosphosites in the region between WWE- and PARP-like-domains are targets for PPKs. Recombinant GST-PPK2 and GST-PPK4 were used together with recombinant GST-RCD1 protein in *in vitro* kinase assays. GST-PPK2 and 4 (asterisks) showed activity towards GST-RCD1 (red arrowhead). There was no activity detected against the mutated GST-RCD1$^{S/T}$IDR2^{A} protein. Upper panel shows autoradiograph, lower panel shows the Coomassie-stained SDS-PAGE.

D. Phosphorylation of IDR2 of RCD1 by PPKs affects its stability and function. *In vivo* abundance of RCD1$^{S/T}$IDR2^{A}-HA and of wild-type RCD1-HA variants was assessed in independent transgenic lines by immunoblot analysis with HA-specific antibody. The RCD1$^{S/T}$IDR2^{A}-HA variant did not fully complement *rcd1*-specific accumulation of alternative oxidases (AOX1/2), as revealed by immunoblot with αAOX1/2 antibodies. Rubisco large subunit detected by amido black staining is shown as a control for equal protein loading.

E. RCD1$^{S/T}$IDR2^{A}-HA variant does not fully complement *rcd1*-specific tolerance to MV. PSII inhibition (Fv/Fm) by MV was measured in indicated lines using 1 µM MV. For each experiment, leaf discs from at least four individual rosettes were used. The experiment was performed three times with similar results. Mean ± SD are shown. *** – P-value < 0.001 with Bonferroni corrected *post hoc* test at the selected time points between *rcd1*: RCD1$^{S/T}$IDR2^{A}-HA (line B) and *rcd1*: RCD1-HA lines. Full source data and statistics are presented in Supplementary table 1.

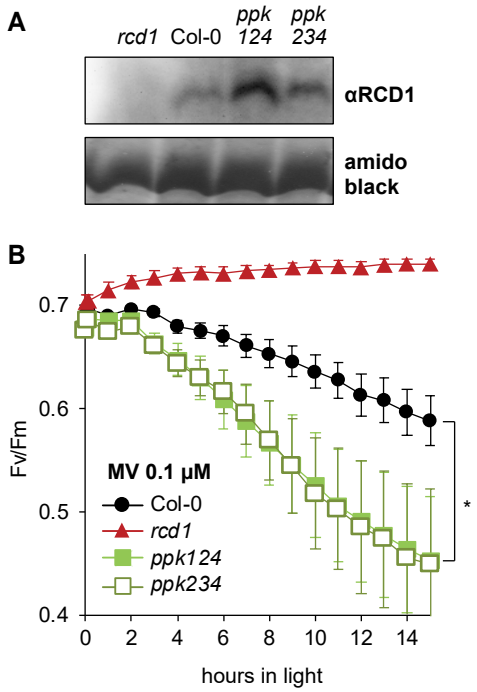

Figure 5. Knockout of PPKs stabilizes native RCD1.

A. RCD1 accumulation in *ppk* triple mutants is higher than in Col-0. RCD1 level was assessed in total protein extracts from 3-week-old plants by immunoblot analysis with RCD1-specific antibody. Rubisco large subunit detected by amido black staining is shown as a control for equal protein loading.

B. *ppk* triple mutants are more sensitive to MV than Col-0. PSII inhibition (Fv/Fm) by MV was measured in indicated lines using 0.1 µM MV. For each experiment, leaf discs from four individual rosettes were used. The experiment was performed three times with similar results. Mean ± SD are shown. * – P-value < 0.05 with Bonferroni corrected *post hoc* test at the selected time point between *ppk124* and Col-0. Source data and statistics are presented in Supplementary table 1.

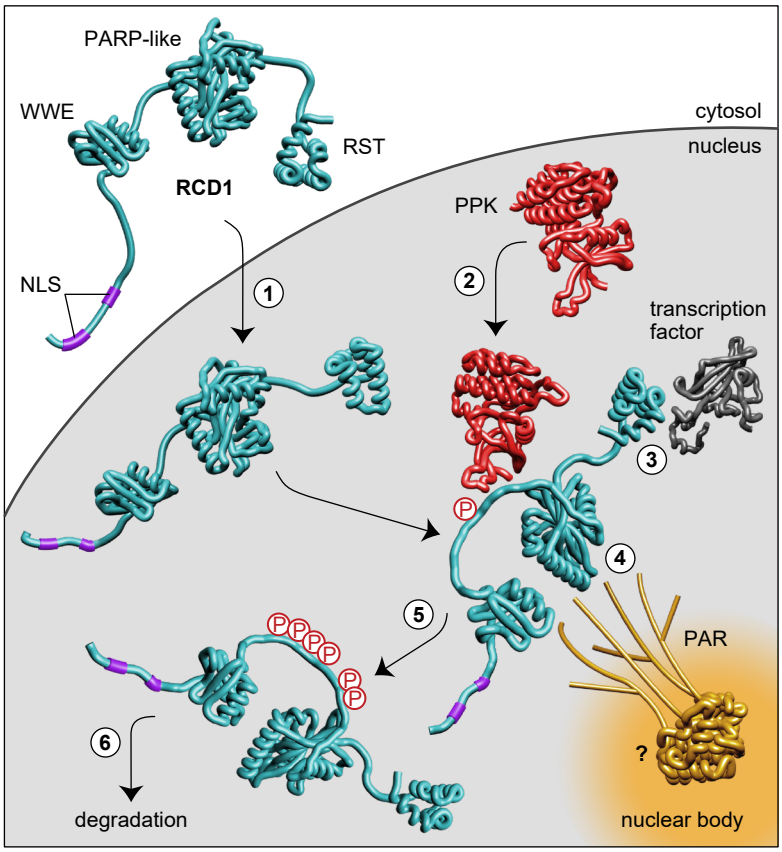

Figure 6. A model describing the regulation of nuclear RCD1 function in dependence of PAR binding and phosphorylation by PPKs.

(1) RCD1 enters the nucleus by means of its bipartite N-terminal NLS sequence. In the nucleus, RCD1 interacts with PPKs (2), with diverse transcription factors (3) and with PAR (4). PAR recruits RCD1 to NBs of yet uncharacterized nature. Unknown PARylated proteins involved in RCD1 recruitment are labeled with a question mark. RCD1 is phosphorylated by PPKs at multiple sites in IDR2 (5), which targets RCD1 for degradation (6). RCD1 structure was predicted in RaptorX (http://raptorx.uchicago.edu/). Structural model of the WWE-domain is based on mouse RNF146 (2RSF), structures of RCD1 PARP-like- (5NGO, Wirthmueller *et al*, 2018) and RST- (5N9Q, Bugge *et al*, 2018) domains have been reported. Terminal and inter-domain regions of RCD1 are not drawn to scale.

Parsed Citations

Adams-Phillips L, Briggs AG, Bent AF. 2010. Disruption of poly(ADP-ribosyl)ation mechanisms alters responses of Arabidopsis to biotic stress. Plant Physiology 152:267–280
Pubmed: Author and Title
Google Scholar: Author Only Title Only Author and Title

Ahel I, Ahel D, Matsusaka T, Clark AJ, Pines J, Boulton SJ, West SC. 2008. Poly(ADP-ribose)-binding zinc finger motifs in DNA repair/checkpoint proteins. Nature 451:81–85.
Pubmed: Author and Title
Google Scholar: Author Only Title Only Author and Title

Ahlfors R, Lång S, Overmyer K, Jaspers P, Brosché M, Tauriainen A, Kollist H, Tuominen H, Belles-Boix E, Piippo M et al. 2004. Arabidopsis RADICAL-INDUCED CELL DEATH1 belongs to the WWE protein-protein interaction domain protein family and modulates abscisic acid, ethylene, and methyl jasmonate responses. Plant Cell 16:1925-1937.
Pubmed: Author and Title
Google Scholar: Author Only Title Only Author and Title

Aravind L. 2001. The WWE domain: a common interaction module in protein ubiquitination and ADP ribosylation. Trends in Biochemical Sciences 26:273-275.
Pubmed: Author and Title
Google Scholar: Author Only Title Only Author and Title

Babiychuk E, Cottrill PB, Storozhenko S, Fuangthong M, Chen Y, O'Farrell MK, Van Montagu M, Inzé D, Kushnir S. 1998. Higher plants possess two structurally different poly(ADP-ribose) polymerases. The Plant Journal 15:635-645.
Pubmed: Author and Title
Google Scholar: Author Only Title Only Author and Title

Bah A, Forman-Kay JD. 2016. Modulation of intrinsically disordered protein function by post-translational modifications. Journal of Biological Chemistry 291:6696-6705.
Pubmed: Author and Title
Google Scholar: Author Only Title Only Author and Title

Briggs AG, Bent AF. 2011. Poly(ADP-ribosyl)ation in plants. Trends in Plant Science 16:372–380.
Pubmed: Author and Title
Google Scholar: Author Only Title Only Author and Title

Brosché M, Blomster T, Salojärvi J, Cui F, Sipari N, Leppälä J, Lamminmäki A, Tomai G, Narayanasamy S, Reddy RA et al. 2014. Transcriptomics and functional genomics of ROS-induced cell death regulation by RADICAL-INDUCED CELL DEATH1. PLoS Genetics 10:e1004112.
Pubmed: Author and Title
Google Scholar: Author Only Title Only Author and Title

Bugge K, Staby L, Kemplen KR, O'Shea C, Bendsen SK, Jensen MK, Olsen JG, Skriver K, Kragelund BB. 2018. Structure of Radical-Induced Cell Death1 hub domain reveals a common αα-scaffold for disorder in transcriptional networks. Structure 26:734-746.
Pubmed: Author and Title
Google Scholar: Author Only Title Only Author and Title

Chen C, Masi R, Lintermann R, Wirthmueller L. 2018. Nuclear import of Arabidopsis poly(ADP-ribose) polymerase 2 is mediated by importin-α and a nuclear localization sequence located between the predicted SAP domains. Frontiers in Plant Science 9:1581.
Pubmed: Author and Title
Google Scholar: Author Only Title Only Author and Title

Chen HH, Qu L, Xu ZH, Zhu JK, Xue HW. 2018. EL1-like casein kinases suppress ABA signaling and responses by phosphorylating and destabilizing the ABA receptors PYR/PYLs in Arabidopsis. Molecular Plant 11:706-719.
Pubmed: Author and Title
Google Scholar: Author Only Title Only Author and Title

Christensen LF, Staby L, Bugge K, O'Shea C, Kragelund BB, Skriver K. 2019. Evolutionary conservation of the intrinsic disorder-based Radical-Induced Cell Death1 hub interactome. Scientific Reports 9:18927.
Pubmed: Author and Title
Google Scholar: Author Only Title Only Author and Title

Christians MJ, Gingerich DJ, Hua Z, Lauer TD, Vierstra RD. 2012. The light-response BTB1 and BTB2 proteins assemble nuclear ubiquitin ligases that modify phytochrome B and D signaling in Arabidopsis. Plant Physiology 160:118-134.
Pubmed: Author and Title
Google Scholar: Author Only Title Only Author and Title

Cohen MS, Chang P. 2018. Insights into the biogenesis, function, and regulation of ADP-ribosylation. Nature Chemical Biology 14:236-243.
Pubmed: Author and Title
Google Scholar: Author Only Title Only Author and Title

DaRosa PA, Wang Z, Jiang X, Pruneda JN, Cong F, Klevit RE, Xu W. 2015. Allosteric activation of the RNF146 ubiquitin ligase by a

poly(ADP-ribosyl)ation signal. Nature 517:223-226.
Pubmed: Author and Title
Google Scholar: Author Only Title Only Author and Title

Favero DS. 2020. Mechanisms regulating PIF transcription factor activity at the protein level.

Physiologia Plantarum. doi: 10.1111/ppl.13075.
Pubmed: Author and Title
Google Scholar: Author Only Title Only Author and Title

Feng B, Liu C, de Oliveira MV, Intorne AC, Li B, Babilonia K, de Souza Filho GA, Shan L, He P. 2015. Protein poly(ADP-ribosyl)ation regulates Arabidopsis immune gene expression and defense responses. PLoS Genetics 11:e1004936
Pubmed: Author and Title
Google Scholar: Author Only Title Only Author and Title

Feng B, Ma S, Chen S, Zhu N, Zhang S, Yu B, Yu Y, Le B, Chen X, Dinesh-Kumar SP et al. 2016. PARylation of the Forkhead-associated domain protein DAWDLE regulates plant immunity. EMBO Reports 17:1799-1813.
Pubmed: Author and Title
Google Scholar: Author Only Title Only Author and Title

Fujibe T, Saji H, Arakawa K, Yabe N, Takeuchi Y, Yamamoto KT. 2004. A methyl viologen-resistant mutant of Arabidopsis, which is allelic to ozone-sensitive rcd1, is tolerant to supplemental ultraviolet-B irradiation. Plant Physiology 134:275-285.
Pubmed: Author and Title
Google Scholar: Author Only Title Only Author and Title

Gupte R, Liu Z, Kraus WL. 2017. PARPs and ADP-ribosylation: recent advances linking molecular functions to biological outcomes. Genes & Development 31:101-126.
Pubmed: Author and Title
Google Scholar: Author Only Title Only Author and Title

Hiltscher H, Rudnik R, Shaikhali J, Heiber I, Mellenthin M, Meirelles Duarte I, Schuster G, Kahmann U, Baier M. 2014. The radical induced cell death protein 1 (RCD1) supports transcriptional activation of genes for chloroplast antioxidant enzymes. Frontiers in Plant Science 5:475.
Pubmed: Author and Title
Google Scholar: Author Only Title Only Author and Title

Huang H, Alvarez S, Bindbeutel R, Shen Z, Naldrett MJ, Evans BS, Briggs SP, Hicks LM, Kay SA, Nusinow DA. 2016. Identification of Evening complex associated proteins in Arabidopsis by affinity purification and mass spectrometry. Molecular and Cellular Proteomics 15:201-217.
Pubmed: Author and Title
Google Scholar: Author Only Title Only Author and Title

Iakoucheva LM, Radivojac P, Brown CJ, O'Connor TR, Sikes JG, Obradovic Z, Dunker AK. 2004. The importance of intrinsic disorder for protein phosphorylation. Nucleic Acids Research 32:1037-1049.
Pubmed: Author and Title
Google Scholar: Author Only Title Only Author and Title

Jaspers P, Blomster T, Brosché M, Salojärvi J, Ahlfors R, Vainonen JP, Reddy RA, Immink R, Angenent G, Turck F et al. 2009. Unequally redundant RCD1 and SRO1 mediate stress and developmental responses and interact with transcription factors. The Plant Journal 60:268-279.
Pubmed: Author and Title
Google Scholar: Author Only Title Only Author and Title

Jaspers P, Overmyer K, Wrzaczek M, Vainonen JP, Blomster T, Salojärvi J, Reddy RA, Kangasjärvi J. 2010. The RST and PARP-like domain containing SRO protein family: analysis of protein structure, function and conservation in land plants. BMC Genomics 11:170.
Pubmed: Author and Title
Google Scholar: Author Only Title Only Author and Title

Jespersen N, Barbar E. 2020. Emerging Features of Linear Motif-Binding Hub Proteins. Trends in Biochemical Sciences 45:375-384.
Pubmed: Author and Title
Google Scholar: Author Only Title Only Author and Title

Jungmichel S, Rosenthal F, Altmeyer M, Lukas J, Hottiger MO, Nielsen ML. 2013. Proteome-wide identification of poly(ADP-Ribosyl)ation targets in different genotoxic stress responses. Molecular Cell 52:272–285.
Pubmed: Author and Title
Google Scholar: Author Only Title Only Author and Title

Karimi M, Inzé D, Depicker A. 2002. GATEWAY vectors for Agrobacterium-mediated plant transformation. Trends in Plant Science 7:193-195.
Pubmed: Author and Title
Google Scholar: Author Only Title Only Author and Title

Kim DS, Challa S, Jones A, Kraus WL. 2020. PARPs and ADP-ribosylation in RNA biology: from RNA expression and processing to protein translation and proteostasis. Genes & Development 34:302-320.
Pubmed: Author and Title

Google Scholar: Author Only Title Only Author and Title

Kragelund BB, Jensen MK, Skriver K. 2012. Order by disorder in plant signaling. Trends in Plant Science 17:625-32.
Pubmed: Author and Title
Google Scholar: Author Only Title Only Author and Title

Lamb RS, Citarelli M, Teotia S. 2012. Functions of the poly(ADP-ribose) polymerase superfamily in plants. Cellular and Molecular Life Sciences 69:175–189.
Pubmed: Author and Title
Google Scholar: Author Only Title Only Author and Title

Leung AKL. 2017. PARPs. Current Biology 27:R1256-R1258.
Pubmed: Author and Title
Google Scholar: Author Only Title Only Author and Title

Liu Q, Wang Q, Deng W, Wang X, Piao M, Cai D, Li Y, Barshop WD, Yu X, Zhou T et al. 2017. Molecular basis for blue light-dependent phosphorylation of Arabidopsis cryptochrome 2. Nature Communications 8:15234.
Pubmed: Author and Title
Google Scholar: Author Only Title Only Author and Title

Love AJ, Yu C, Petukhova NV, Kalinina NO, Chen J, Taliansky ME. 2017. Cajal bodies and their role in plant stress and disease responses. RNA Biology 14:779-790.
Pubmed: Author and Title
Google Scholar: Author Only Title Only Author and Title

Mao YS, Zhang B, Spector DL. 2011. Biogenesis and function of nuclear bodies. Trends in Genetics 27:295-306.
Pubmed: Author and Title
Google Scholar: Author Only Title Only Author and Title

Martello R, Leutert M, Jungmichel S, Bilan V, Larsen SC, Young C, Hottiger MO, Nielsen ML. 2016. Proteome-wide identification of the endogenous ADP-ribosylome of mammalian cells and tissue. Nature Communications 7:12917.
Pubmed: Author and Title
Google Scholar: Author Only Title Only Author and Title

Martín G, Leivar P, Ludevid D, Tepperman JM, Quail PH, Monte E. 2016. Phytochrome and Retrograde Signalling Pathways Converge to Antagonistically Regulate a Light-Induced Transcriptional Network. Nature Communications 7:11431.
Pubmed: Author and Title
Google Scholar: Author Only Title Only Author and Title

McLellan H, Boevink PC, Armstrong MR, Pritchard L, Gomez S, Morales J, Whisson SC, Beynon JL, Birch PR. 2013. An RxLR effector from Phytophthora infestans prevents re-localisation of two plant NAC transcription factors from the endoplasmic reticulum to the nucleus. PLoS Pathogens 9:e1003670.
Pubmed: Author and Title
Google Scholar: Author Only Title Only Author and Title

Mergner J, Frejno M, List M, Papacek M, Chen X, Chaudhary A, Samaras P, Richter S, Shikata H, Messerer M et al. 2020. Mass-spectrometry-based draft of the Arabidopsis proteome. Nature 579:409-414.
Pubmed: Author and Title
Google Scholar: Author Only Title Only Author and Title

Nakagawa T, Suzuki T, Murata S, Nakamura S, Hino T, Maeo K, Tabata R, Kawai T, Tanaka K, Niwa Y et al. 2007. Improved Gateway binary vectors: high-performance vectors for creation of fusion constructs in transgenic analysis of plants. Bioscience Biotechnology, and Biochemistry 71: 2095-2100.
Pubmed: Author and Title
Google Scholar: Author Only Title Only Author and Title

Ni W, Xu SL, Gonzalez-Grandio E, Chalkley RJ, Huhmer AFR, Burlingame AL, Wang ZY, Quail PH. 2017. PPKs mediate direct signal transfer from phytochrome photoreceptors to transcription factor PIF3. Nature Communications 8:15236.
Pubmed: Author and Title
Google Scholar: Author Only Title Only Author and Title

O'Shea C, Staby L, Bendsen SK, Tidemand FG, Redsted A, Willemoës M, Kragelund BB, Skriver K. 2017. Structures and short linear motif of disordered transcription factor regions provide clues to the interactome of the cellular hub protein Radical-induced Cell Death1. Journal of Biological Chemistry 292:512-527.
Pubmed: Author and Title
Google Scholar: Author Only Title Only Author and Title

Overmyer K, Tuominen H, Kettunen R, Betz C, Langebartels C, Sandermann H Jr, Kangasjärvi J. 2000. Ozone-sensitive Arabidopsis rcd1 mutant reveals opposite roles for ethylene and jasmonate signaling pathways in regulating superoxide-dependent cell death. Plant Cell 12:1849-1862.
Pubmed: Author and Title
Google Scholar: Author Only Title Only Author and Title

Palazzo L, Leidecker O, Prokhorova E, Dauben H, Matic I, Ahel I. 2018. Serine is the major residue for ADP-ribosylation upon DNA damage. Elife 7: e34334.

Pubmed: Author and Title
Google Scholar: Author Only Title Only Author and Title

Qin F, Sakuma Y, Tran LS, Maruyama K, Kidokoro S, Fujita Y, Fujita M, Umezawa T, Sawano Y, Miyazono K et al. 2008. Arabidopsis DREB2A-interacting proteins function as RING E3 ligases and negatively regulate plant drought stress-responsive gene expression. Plant Cell 20, 1693–1707.
Pubmed: Author and Title
Google Scholar: Author Only Title Only Author and Title

Reddy AS, Day IS, Göhring J, Barta A. 2012. Localization and dynamics of nuclear speckles in plants. Plant Physiology 158:67-77.
Pubmed: Author and Title
Google Scholar: Author Only Title Only Author and Title

Saidi Y, Hearn TJ, Coates JC. 2012. Function and evolution of 'green' GSK3/Shaggy-like kinases. Trends in Plant Science 17:39-46.
Pubmed: Author and Title
Google Scholar: Author Only Title Only Author and Title

Shapiguzov A, Vainonen JP, Hunter K, Tossavainen H, Tiwari A, Järvi S, Hellman M, Aarabi F, Alseekh S, Wybouw B et al. 2019. Arabidopsis RCD1 coordinates chloroplast and mitochondrial functions through interaction with ANAC transcription factors. Elife 8: e43284.
Pubmed: Author and Title
Google Scholar: Author Only Title Only Author and Title

Siligato R, Wang X, Yadav SR, Lehesranta S, Ma G, Ursache R, Sevilem I, Zhang J, Gorte M, Prasad K et al. 2016. MultiSite Gateway-compatible cell type-specific gene-inducible system for plants. Plant Physiology 170: 627-641.
Pubmed: Author and Title
Google Scholar: Author Only Title Only Author and Title

Simon L, Voisin M, Tatout C, Probst AV. 2015. Structure and function of centromeric and pericentromeric heterochromatin in Arabidopsis thaliana. Frontiers in Plant Science 6:1049.
Pubmed: Author and Title
Google Scholar: Author Only Title Only Author and Title

Song J, Keppler BD, Wise RR, Bent AF. 2015. PARP2 Is the predominant poly(ADP-Ribose) polymerase in Arabidopsis DNA damage and immune responses. PLoS Genetics 11:e1005200.
Pubmed: Author and Title
Google Scholar: Author Only Title Only Author and Title

Stampfl H, Fritz M, Dal Santo S, Jonak C. 2016. The GSK3/Shaggy-Like Kinase ASKα Contributes to Pattern-Triggered Immunity. Plant Physiology 171:1366-1377.
Pubmed: Author and Title
Google Scholar: Author Only Title Only Author and Title

Su Y, Wang S, Zhang F, Zheng H, Liu Y, Huang T, Ding Y. 2017. Phosphorylation of histone H2A at Serine 95: a plant-specific mark involved in flowering time regulation and H2A.Z deposition. Plant Cell 29:2197-2213.
Pubmed: Author and Title
Google Scholar: Author Only Title Only Author and Title

Teloni F, Altmeyer M. 2016. Readers of poly(ADP-ribose): designed to be fit for purpose. Nucleic Acids Research 44:993-1006.
Pubmed: Author and Title
Google Scholar: Author Only Title Only Author and Title

Teotia S, Lamb RS. 2009. The paralogous genes RADICAL-INDUCED CELL DEATH1 and SIMILAR TO RCD ONE1 have partially redundant functions during Arabidopsis development. Plant Physiology 151:180-198.
Pubmed: Author and Title
Google Scholar: Author Only Title Only Author and Title

Vainonen JP, Jaspers P, Wrzaczek M, Lamminmäki A, Reddy RA, Vaahtera L, Brosché M, Kangasjärvi J. 2012. RCD1-DREB2A interaction in leaf senescence and stress responses in Arabidopsis thaliana. Biochemical Journal 442:573-581.
Pubmed: Author and Title
Google Scholar: Author Only Title Only Author and Title

Vainonen JP, Shapiguzov A, Vaattovaara A, Kangasjärvi J. 2016. Plant PARPs, PARGs and PARP-like proteins. Current Protein and Peptide Science 17:713-723.
Pubmed: Author and Title
Google Scholar: Author Only Title Only Author and Title

Van Buskirk EK, Decker PV, Chen M. 2012. Photobodies in light signaling. Plant Physiology 158:52-60.
Pubmed: Author and Title
Google Scholar: Author Only Title Only Author and Title

Wang Z, Michaud GA, Cheng Z, Zhang Y, Hinds TR, Fan E, Cong F, Xu W. 2012. Recognition of the iso-ADP-ribose moiety in poly(ADP-ribose) by WWE domains suggests a general mechanism for poly(ADP-ribosyl)ation-dependent ubiquitination. Genes & Development 26:235-240.
Pubmed: Author and Title

Google Scholar: Author Only Title Only Author and Title

Wang Z, Casas-Mollano JA, Xu J, Riethoven JJ, Zhang C, Cerutti H. 2015. Osmotic stress induces phosphorylation of histone H3 at threonine 3 in pericentromeric regions of Arabidopsis thaliana. Proceedings of the National Academy of Sciences, USA 112:8487-8492.
Pubmed: Author and Title
Google Scholar: Author Only Title Only Author and Title

Wirthmueller L, Asai S, Rallapalli G, Sklenar J, Fabro G, Kim DS, Lintermann R, Jaspers P, Wrzaczek M, Kangasjärvi J et al. 2018. Arabidopsis downy mildew effector HaRxL106 suppresses plant immunity by binding to RADICAL-INDUCED CELL DEATH1. New Phytologist 220:232-248.
Pubmed: Author and Title
Google Scholar: Author Only Title Only Author and Title

Zhang Y, Liu S, Mickanin C, Feng Y, Charlat O, Michaud GA, Schirle M, Shi X, Hild M, Bauer A et al. 2011. RNF146 is a poly(ADP-ribose)-directed E3 ligase that regulates axin degradation and Wnt signalling. Nature Cell Biology 13:623-629.
Pubmed: Author and Title
Google Scholar: Author Only Title Only Author and Title

Zhang YJ, Wang JQ, Ding M, Yu YH. 2013. Site-specific characterization of the Asp- and Glu-ADP-ribosylated proteome. Nature Methods 10:981–984.
Pubmed: Author and Title
Google Scholar: Author Only Title Only Author and Title

Zheng H, Zhang F, Wang S, Su Y, Ji X, Jiang P, Chen R, Hou S, Ding Y. 2018. MLK1 and MLK2 coordinate RGA and CCA1 to regulate hypocotyl elongation in Arabidopsis thaliana. Plant Cell 30:67-82.
Pubmed: Author and Title
Google Scholar: Author Only Title Only Author and Title